



Università
Ca' Foscari
Venezia

**Scuola Dottorale di Ateneo
Graduate School**

**Dottorato di ricerca
in Economics
Ciclo 29°
Anno di discussione 2017**

***Analysing the Evolution of Violent Phenomena
with Agent-Based Models and Non-Parametric
Statistics***

**SETTORE SCIENTIFICO DISCIPLINARE DI AFFERENZA: SECS-S/06
Tesi di Dottorato di Alessandro Moro, matricola 956079**

Coordinatore del Dottorato

Prof. Giacomo Pasini

Tutore del Dottorando

Prof. Paolo Pellizzari

Co-tutore del Dottorando

Prof. Stefano Magrini

Analysing the Evolution of Violent
Phenomena with Agent-Based Models and
Non-Parametric Statistics

Alessandro Moro

Abstract

In the present PhD dissertation different phenomena of political and civil violence are analysed using quantitative methods. In particular, the first chapter of the thesis develops an agent-based model which is able to provide an explanation for the multiplicity of political scenarios emerged after the Arab Spring: the successful revolution in Tunisia, the failed protests in Saudi Arabia and Bahrain, and civil war in Syria and Libya. The second chapter evaluates the effects of gun availability on homicides with an agent-based model: in the analysis conditions are derived under which the number of deaths is minimised with restrictions on gun possession or, vice versa, with a diffused gun ownership. In the third chapter, using crime data for the US states and the distribution dynamics approach, two distinct phases are detected in the evolution of the property crime distribution: a period of convergence (1971-1980) is followed by a tendency towards bimodality (1981-2010). Moreover, the analysis reveals that differences in income and police can explain the emergence of this shape.

Contents

Introduction	13
1 An Agent-Based Model of Revolutions	19
1.1 Introduction	20
1.2 The Model	23
1.3 Model Results	29
1.4 Global Sensitivity Analysis	36
1.5 Stationarity and Ergodicity	40
1.6 Discussion	43
2 Gun Availability and Violence	47
2.1 Introduction	48
2.2 The Model	50
2.2.1 A Theoretical Framework	51
2.2.2 The Agent-Based Extension	53
2.3 Results	56
2.3.1 Homicides Committed and Gun Availability	58
2.3.2 Police versus Self-Defense	59
2.3.3 The Other Factors	61
2.3.4 Variability of Homicides	62
2.3.5 The Effect of Spatial Concentration	64
2.3.6 More Sophisticated Interactions	66
2.4 Concluding Remarks	66

3	Property Crime Distribution in the US	69
3.1	Introduction	70
3.2	A Two-Region Model of Crime Dynamics	72
3.3	Methodology	78
3.3.1	Distribution Dynamics Approach	79
3.3.2	Criticisms of Other Approaches	81
3.4	Data	82
3.5	Distribution Dynamics of Property Crime	86
3.6	Robustness Checks	88
3.7	Conditional Distribution Dynamics	93
3.8	Concluding Remarks	98
	Acknowledgments	103
	Bibliography	105

List of Figures

1.1	The three model outcomes.	31
1.2	Average proportion of policemen killed for different values of the two precision parameters.	34
1.3	Variability of the proportion of policemen killed for different values of the two precision parameters.	35
1.4	The unpredictability of revolutions.	37
1.5	Probability of killing a policeman as a function of the revolutionaries' threshold.	40
1.6	Stationary and ergodic properties of the model	42
2.1	Number of homicides committed for different values of gun availability and different numbers of police officers in the baseline scenario (experiment 1).	59
2.2	Number of homicides committed for different values of gun availability and different numbers of police officers in the larger space scenario (experiment 2).	60
2.3	Difference between killings performed by police officers and those committed for self-defense in correspondence to different values of gun availability and different numbers of police officers in the baseline scenario (experiment 1).	61

2.4	Number of homicides committed for different values of gun availability and different numbers of police officers in the baseline, high precision, low lifetime and high violence scenarios (experiments 1, 3, 4, 5).	62
2.5	Variability of homicides committed for different values of gun availability and different numbers of police officers in the baseline scenario (experiment 1).	63
2.6	Variability of homicides committed for different values of gun availability and different numbers of police officers in the baseline, high precision, low lifetime and high violence scenarios (experiments 1, 3, 4, 5).	64
2.7	Number of homicides committed for different values of gun availability when agents are spatially concentrated and when they are randomly located in the bidimensional space.	65
2.8	Total number of killings perpetrated by killers and by non-violent citizens for self-defense with more realistic interactions and different self-defense abilities.	67
3.1	Time series of the main variables of the model in the presence of different income shocks.	77
3.2	Time series of the property crime rate in the US from 1971 to 2010.	83
3.3	Moran scatterplot map and significance map of property crime rates in 1971 and 2010.	85
3.4	Distribution dynamics analysis of property crime rates for the period 1971-2010 using the 48 continental US states.	87
3.5	Distribution dynamics analysis of property crime rates for the period 1971-1980 using the 48 continental US states.	89
3.6	Distribution dynamics analysis of property crime rates for the period 1981-2010 using the 48 continental US states.	90

3.7	Distribution dynamics analysis of property crime rates for the period 1971-1980 using the 9 US regions.	91
3.8	Distribution dynamics analysis of property crime rates for the period 1981-2010 using the 9 US regions.	92
3.9	Distribution dynamics analysis of real per capita personal income for the period 1981-2010 using the 48 continental US states.	94
3.10	Distribution dynamics analysis of state police employees per 100,000 inhabitants for the period 1981-2010 using the 48 continental US states.	95
3.11	Distribution dynamics analysis of property crime rates for the period 1971-2010 conditioning on income and police. . .	99
3.12	Distribution dynamics analysis of property crime rates for the period 1981-2010 conditioning on income and police. . .	100

List of Tables

1.1	Parameter values fixed in all model simulations.	29
1.2	Estimates of the statistical models.	39
2.1	Values chosen for the main parameters of the model in the five experiments performed.	57
3.1	Values chosen for the parameters of the model.	76
3.2	Conditioning regressions.	97

Introduction

In the Preface to the *Phenomenology of Mind*, Hegel (1807 [1910], page 17) famously wrote: “The truth is the whole. The whole, however, is merely the essential nature reaching its completeness through the process of its own development.”

This sentence captures well the essence of the present PhD dissertation, which illustrates several applications of two, very different, methodologies that have in common the attempt of overcoming, in their respective domains, the limitations of the representative agent dogma, allowing the study of the emergent properties of complex systems with heterogeneous players. These two approaches are the agent-based modeling and the distribution dynamics method. Both have been employed in this work to analyse three phenomena of civil and political violence whose study can benefit from the adoption of new methods. These phenomena are: the Arab Spring revolution, the relationship between gun diffusion and violence, and the evolution of the distribution of property crime across the US states.

As pointed out by Hartley (1996), since the Marshall’s *Principles of Economics* (1920 [1961]), the mainstream economic literature has been dominated by the idea of the “representative agent”. However, although this concept has been harshly criticised, such as in Kirman (1992), it is still the dominant paradigm in many economic fields. As noted in Hartley (1996, page 176), the main criticism consists in the difficulty “to give a consistent and empirically usable definition of what a representative individual is like. If we create an agent that is some sort of statistical average, the model using

it will not necessarily explain aggregate data. If we try to define the representative agent as the marginal purchaser, it becomes a will-o'-the-wisp whose taste parameters are endogenously determined by market characteristics.” Moreover, in the most favourable situation in which we can construct a representative agent whose utility-maximizing choices correspond to those of the population, Kirman (1992, page 123) stresses that “even in this case the representative agent can lead to misleading policy analyses”, because we have no assurance that the choice of the representative agent will coincide with the aggregate choice of the population after the policy change.

In order to overcome these limitations, the agent-based literature presents many models in which multiple and heterogeneous agents take their decisions following simple behavioural rules and interacting with their peers over time and, possibly, across different spatial units. Researchers usually specify intuitive and behaviourally plausible heuristics for each agent and observe the emergence of regular, aggregate behaviours from the repeated interactions of these players. In the First and Second Chapter of the present thesis we decide to follow this approach to study two different phenomena related to political and civil violence: the Arab Spring revolutions and the impact of weapon diffusion on the number of homicides committed.

Another field dominated by the paradigm of the “representative unit” is the empirical analysis of convergence. In this framework the mainstream approach is represented by the beta-convergence (Baumol, 1986; Barro, 1991; Barro and Sala-i-Martin, 1991, 1992) and sigma-convergence analysis (Sala-i-Martin, 1996). Essentially, the beta-convergence aims at testing the convergence of a given process by looking at a negative correlation between the initial values of the studied variable and its growth rates: if statistical units with high values in the initial period show lower growth rates than units with low values, this should mean that they converge to a common steady state. However, it has been recognised that a negative relationship between initial values and growth rates is a necessary but not a sufficient

condition for convergence (Quah, 1993a): this is precisely due to the fact that, by focusing on the behaviour of a representative unit towards its own steady state, the beta-convergence analysis is completely silent on what happens to the entire cross-sectional distribution of the studied statistical units. Thus, it has been suggested to complement the beta-convergence approach with the study of the cross-sectional variability over time (sigma-convergence): the idea is that a reduction of the standard deviation of the distribution, together with a negative relationship between initial values and growth rates, should be a sufficient signal of convergence among the units of interest. Indeed, as argued by Quah (1996a), a constant variability is compatible with very different behaviours, from criss-crossing and leap-frogging to persistent inequality. Distinguishing between these completely different dynamics is crucial and it is possible only by analysing the entire cross-sectional distribution.

The distribution dynamics methodology (Quah, 1993a and b, 1996a and b, 1997) has been proposed as an alternative and more meaningful way to analyse convergence: in fact, this approach allows the study of the entire cross-sectional distribution of a given variable, both in terms of external shape and intra-distributional dynamics, using stochastic kernels to describe its evolution over time. This method has been adopted in the Third Chapter to study the evolution of property crime rates across the 48 conterminous and continental US states over the period 1971-2010.

In particular, this PhD dissertation is organised in three chapters. The first one¹ develops an agent-based computational model of violent political revolutions in which a subjugated population of citizens and an armed revolutionary organisation attempt to overthrow a central authority and its loyal forces. The model replicates several patterns of rebellion consistent with major historical revolutions, and provides an explanation for the mul-

¹This chapter has been published in PLoS ONE as: Moro, A. (2016). "Understanding the Dynamics of Violent Political Revolutions in an Agent-Based Framework." PLoS ONE, 11(4): e0154175.

tiplicity of outcomes that can arise from an uprising. The relevance of the heterogeneity of scenarios simulated by the model can be understood by considering the recent experience of the Arab Spring involving several rebellions that arose in an apparently similar way, but resulted in completely different political outcomes: the successful revolution in Tunisia, the failed protests in Saudi Arabia and Bahrain, and civil war in Syria and Libya.

The aim of the Second Chapter is the evaluation of the effects of gun availability on firearm-related homicides in an agent-based framework. Behind this relationship there is a likely trade-off: on the one hand, a diffused gun ownership can protect victims against the attacks of violent individuals; on the other hand, a higher diffusion of weapons increases the probability that a violent individual can obtain a gun. The analysis of this chapter reveals that, with a high number of police officers relative to the space and the number of citizens, it is possible to minimise the number of homicides either with a complete ban of weapons or with a capillary diffusion of guns. Conversely, when the number of police officers is relatively low, only a policy that reduces gun availability close to zero minimises the firearm-related deaths. Moreover, a greater presence of policemen generates a transition from a private kind of self-defense to a public one.

Finally, in the Third Chapter,² using crime data for the 48 continental and conterminous US states and the distribution dynamics approach, this paper detects two distinct phases in the evolution of the property crime distribution: a period of strong convergence (1971-1980) is followed by a tendency towards divergence and bimodality (1981-2010). The analysis also reveals that differences in income per capita and number of police officers can explain the emergence of a bimodal shape in the distribution of property crime rates: in fact, after conditioning on these variables, the bimodality completely disappears. This empirical evidence is consistent with the

²A slightly smaller version of this chapter has been published (published online before print) in *Urban Studies* as: Moro, A. (2016). "Distribution Dynamics of Property Crime Rates in the United States." *Urban Studies*, doi:10.1177/0042098016652535.

predictions of a two-region model, that stresses the importance of income inequality in determining the dynamics of the property crime distribution.

Chapter 1

Understanding the Dynamics of Violent Political Revolutions in an Agent-Based Framework

Abstract

This chapter develops an agent-based computational model of violent political revolutions in which a subjugated population of citizens and an armed revolutionary organisation attempt to overthrow a central authority and its loyal forces. The model replicates several patterns of rebellion consistent with major historical revolutions, and provides an explanation for the multiplicity of outcomes that can arise from an uprising. The heterogeneity of scenarios generated by the model is a relevant feature whose importance can be understood by considering the recent experience of the Arab Spring involving several rebellions that arose in an apparently similar way, but resulted in completely different political outcomes: the successful revolution in Tunisia, the failed protests in Saudi Arabia and Bahrain, and civil war in Syria and Libya.

1.1 Introduction

The phenomenon of political revolutions has once again caught the attention of researchers in the wake of the recent wave of uprisings in the Arab World. The main purpose of this chapter is to present an agent-based computational model that outlines the common dynamics of major political revolutions and replicates a number of stylised facts.

The model features three types of agent that interact in a bidimensional torus space: a population of citizens who are oppressed by a central government; members of a revolutionary organisation who attempt to overthrow the government by an armed uprising; and loyal policemen who are tasked with suppressing the rebellion.

This simple model is able to reproduce several patterns of rebellion consistent with major historical revolutions: a pre-revolutionary period characterised by spontaneous riots, motivated mainly by poor economic conditions and social inequality, gives way to an actual revolutionary rebellion, in which organised elements mobilise popular masses against the central government.

Moreover, the model provides an explanation for the multiplicity of outcomes that can arise from an uprising: a completely successful revolution leading to the overthrow of the central authority; a failed rebellion followed by a return to the status quo; an intermediate case where the uprising is unable to change the political system, but is sufficiently strong to destabilise the country and drive it towards anarchy.

The heterogeneity of scenarios generated by the model is a relevant feature whose importance can be understood by considering the recent experience of the Arab Spring involving several rebellions that arose in an apparently similar way, but resulted in completely different political outcomes: e.g. the successful revolution in Tunisia, the failed protests in Saudi Arabia and Bahrain, and civil war in Syria and Libya.

For decades, the most popular conceptualisations of revolution were the

Marxian theory and the relative deprivation theory. The former emphasises the role of changes in production methods in generating discontent and rebellion; the latter focuses on the gap between economic expectations and realised economic performances to explain the sense of frustration and, consequently, riot participation. Both theories establish an automatic link between the structural conditions that generate grievance in society and the likelihood of revolutionary episodes. Moreover, in both theories participation in rebellion is motivated by a collective good argument, such as the desire to change the oppressive social order. Two of the most influential scholars in this stream of literature are Skocpol (1979) with regard to the Marxian theory and Davies (1962) concerning the relative deprivation theory. For a complete review of the political science literature about revolutions, see Goldstone (2001).

In contrast, Tullock (1971) develops an economic approach to explain participation in revolutions: since the benefit of an extra unit of public good is small relative to the cost of obtaining it by participating in a rebellion, individuals decide whether or not to participate based on their private gains or losses. Silver (1974) provides a classification of revolutions based on Tullock's theory. Moreover, Kuran (1989, 1991, 1995) criticises the idea of an automatic relationship between social grievance and revolution, arguing that most historical revolutions were unanticipated. He provides an explanation based on the observation that people who dislike their government tend to conceal their political preferences as long as the opposition seems weak. For this reason, regimes that appear to be absolutely stable may experience a sudden loss of support in the event of a minor increase in the size of the opposition, even if triggered by insignificant events.

The economic and political science literature have endeavoured to solve the collective action problems inherent in revolutions. For example, in criticism of Tullock, Lichbach (1994, 1995, 1996) identifies a number of solutions based on sanctioning and group identification methods. These solutions

include the possibility of imposing community obligations, establishing institutional mechanisms, arranging contracts and using authority. For an example of an institutional kind of solution in the context of 18th century merchant sailors, see Leeson (2010).

Furthermore, in line with Kuran's theory, Rubin (2014) argues that cascades of preference revelation are more likely to occur following a major shock in highly centralised regimes. This is because citizens in such political systems have a greater incentive to conceal their true political opinions in order to avoid economic or legal sanctions being imposed by the central authority. Makowsky and Rubin (2013) extend the previous work by developing an agent-based model to study how social network technology favours preference revelation in centralised societies.

A number of game theoretic papers have also been produced that analyse the economic causes of political change: for instance, following Acemoglu and Robinson's (2001) model of the economic origins of democracy, Ellis and Fender (2011) derive conditions under which democracy arises peacefully, when it occurs after a revolution, and when oligarchic governments persist. An alternative view is represented by the paper of Gard-Murray and Bar-Yam (2015), who argue that democracies are more systemically complex than autocracies and, since violent revolutions are likely to disrupt existing evolved complexity, dictatorships have higher chances of emerging after uprisings.

Finally, this paper is also influenced to a great extent by Granovetter's (1978) theory about threshold models of collective behaviours and by Epstein's (2002) agent-based model of civil violence. According to Granovetter, individuals face many situations with multiple alternatives, and the costs and benefits associated with these alternatives depend on how many other individuals have chosen the various options in the past. For this reason, each individual has a personal threshold, and decides to join collective action, such as a riot or a strike, if the number of people participating at that

time exceeds this threshold. Following this idea, Epstein develops an agent-based model of civil violence involving two types of player, agents and cops, interacting in a bidimensional torus space. In this model the agents decide to rebel against the government if their level of grievance corrected by the risk of being arrested by the cops exceeds their activation threshold. One of the main findings of this model is that intermittent outbursts of violence occur, distributed irregularly over time and space. Another study that explores the temporal and spatial diffusion of civil unrest is that produced by Braha (2012). In particular, his paper demonstrates that the distribution of real episodes of civil violence can be replicated using a spatially extended dynamical model that incorporates the effects of social and communication networks.

However, the existing literature does not consider the heterogeneity of scenarios that can result after a revolution. Conversely, the capability of generating multiple post-revolutionary outcomes is a prominent feature of the model presented in this chapter and represents the main motivation of the proposed approach.

The rest of the chapter is organised as follows: next section describes the model; Section 1.3 presents the three outcomes generated by the model and their dependence on the model parameters is highlighted using graphical tools; in Section 1.4 some statistical models are estimated in order to analyse the main features of the simulated data; Section 1.5 studies the emerging outcomes of the model with respect to the categories of stationarity and ergodicity; finally, Section 1.6 discusses the results and their relevance for the analysis of contemporary revolutions.

1.2 The Model

In the agent-based computational model presented in this chapter, there are three types of agent that interact in a bidimensional torus space: citizens,

revolutionaries and policemen. Citizens are members of a population subjugated to a central authority who decide whether or not to rebel against the government based on their degree of economic and political grievance. Revolutionaries are members of an organised opposition group that seeks to overthrow the central government by an armed uprising. Policemen are the forces loyal to the central authority that have been tasked to suppress any kind of revolt by arresting rebellious citizens and killing revolutionaries.

In this section, the features of each agent are described in detail, beginning with the citizen specification. As in Epstein (2002), social grievance represents the motivation that potentially leads citizens to revolt; for each citizen i the grievance is assumed to be the product of an index of economic hardship H and a measure of government illegitimacy, defined as $1 - l$, where l is a parameter measuring the legitimacy of the central authority:

$$G(y_i) = (1 - l) H(y_i) \quad (1.1)$$

In contrast to Epstein's specification, the perceived hardship, and consequently grievance, is a function of citizens' income y_i . In fact, each citizen is endowed with an income drawn from a lognormal distribution:¹

$$y_i \sim \log N(a, b^2) \quad (1.2)$$

The functional form chosen for the hardship index is:

$$H(y_i) = \frac{\exp[E(y_i) - y_i]}{1 + \exp[E(y_i) - y_i]} \quad (1.3)$$

This function allows each citizen's economic condition to be mapped to a value in the $(0, 1)$ interval. This index is a logistic transformation of

¹Although this assumption adds realism to the model with respect to the uniform distribution of hardship in Epstein's model, it does not determine the main results of the following analysis. In fact, alternative distributions of income, such as the normal and the gamma distributions, or the original hardship function in Epstein (2002) qualitatively lead to the same conclusions.

the difference between citizens' income and the expected income in the population $E(y_i) = \exp(a + \frac{b^2}{2})$. Given this monotonic transformation, hardship is a decreasing function of citizens' income.²

On the other hand, the cost of participating in a rebellion is defined as the product of the estimated probability of being arrested A_i and the opportunity cost of joining a revolt J :

$$N(y_i) = A_i J(y_i) \quad (1.4)$$

In fact, each citizen estimates the probability of being arrested before actively joining a rebellion. This estimated probability is defined as in Epstein (2002): it is an increasing function of the ratio of policemen to already rebellious agents inside the citizen's vision radius. In particular, in this model rebel agents can either be citizens and revolutionaries:

$$A_i = 1 - \exp \left[-w_1 \left(\frac{P_i^v}{1 + C_i^v + R_i^v} \right) \right] \quad (1.5)$$

where P_i^v , C_i^v and R_i^v represent the number of policemen, rebellious citizens and active revolutionaries within the citizen's vision, respectively. The vision, a circular neighbourhood with centre located in the citizen's position and a radius equal to v , represents the set of lattice positions probed by the citizen. The one in the previous formula makes explicit that, before participating in a riot, a citizen will count himself as an active agent: thus the ratio is always well defined. In practice, the floor operator is applied to the ratio of policemen to rebel agents, as in Wilensky's (1999) version of Epstein's model.

If an active citizen is arrested by a policeman, he remains in jail for

²This expression is similar to the definition of grievance employed by Kim and Haneman (2011). The main difference with respect to their specification is that the two authors use a local measure of inequality, i.e. the distance between each agent's wage and the average wage in the agent's neighbourhood; conversely, in this model a global measure of inequality is preferred.

a number of periods drawn from a uniform distribution on the $(0, j_{max})$ interval. For this reason, the opportunity cost of rebelling is defined as a function of the maximum number of periods in jail j_{max} , multiplied by income loss whilst in jail:

$$J(y_i) = 2 \frac{\exp[w_2(y_i j_{max})]}{1 + \exp[w_2(y_i j_{max})]} - 1 \quad (1.6)$$

Since the inner argument of the logistic transformation is positive, given that income assumes only positive values, the logistic function is rescaled in order to define a cost function J on the $(0, 1)$ interval. Expression (1.6) is also consistent with the literature on political violence, which finds a negative relationship between income and participation in civil violence phenomena. For example, Collier and Hoeffler (1998, 2004) and Fearon and Laitin (2003), using cross-country regressions, find that economic growth and per capita income correlate negatively with the risk of civil conflict. Moreover, Miguel, Satyanath and Sergenti (2004) identify a causal negative effect between positive income shocks and civil war incidence in Sub-Saharan African countries employing an instrumental variable approach.

Having defined the incentives and the costs underlying participation in riot activities, it is now possible to specify citizens' rule of activation. Citizens particularly become active, meaning that they decide to rebel against the government, if the difference between their social grievance and the expected opportunity cost of joining a riot exceeds a fixed threshold; otherwise, they will keep quiet. The citizens' rule is therefore:

Rule C: if $G(y_i) - N(y_i) > f$ be active; otherwise, keep quiet.

This rule can be interpreted using Kuran's (1989) theory: the left-hand side represents the expected utility of expressing opposition to the central authority in public; the right-hand side f is the constant utility of staying quiet and concealing private political preferences.

The revolutionaries' behaviour is simpler. Revolutionaries are members of an organised group that attempts to overthrow the government by an armed conflict. This kind of agent can be interpreted as a proper revolutionary group or as defected elements from the military that decide to side with the population in revolt. Historical examples of the first type of organisation include the Bourgeois Militia of Paris in the French Revolution (1789); the Bolsheviks and Red Guards in the Russian Revolution (1917); the leftist revolutionaries of the Organisation of Iranian People's Fedai Guerrillas in the Iranian Revolution (1979); the Muslim Brotherhood in the Egyptian Revolution (2011); the jihadist group of the Islamic State of Iraq and the Levant in the Syrian Civil War (2011), and many others. Defections from the military are also very common in all revolutions: a typical example is the pro-Khomeini members of the Iranian Air Force who fought against the loyal Immortal Guards during the 1979 uprisings.

It is assumed that revolutionaries behave according to the following rule:

Rule R: if $\frac{R+C}{P} > n$ be active and kill a randomly selected policeman inside vision radius v with a probability equal to r ; otherwise, remain hidden.

Here R , C and P are the total number of revolutionaries, the total number of active citizens and the total number of policemen, respectively. Rule R means that revolutionaries decide to become active when the ratio of rebel forces to policemen loyal to the government exceeds a given threshold n . In this respect, revolutionaries are different from citizens: citizens choose how to behave according to local information available within their vision radius. In contrast, revolutionaries act on the basis of global information and decide when to start a revolution by employing a threshold-based rule involving the total number of active citizens in the population. In fact, it is assumed that the revolutionary organisation is spread across the country, enabling it to obtain an estimate of the total number of active agents in the

population.

When a revolutionary is active, he kills a randomly selected policeman in his vision radius with a probability equal to r . Otherwise, when the ratio is less than the fixed threshold, all revolutionaries will remain hidden among quiet citizens and policemen will be unable to identify them.

As far as policemen are concerned, they simply inspect the lattice positions inside their vision radius and randomly choose an active citizen or active revolutionary: if the randomly selected agent is a citizen, the policeman will arrest him, or will kill him if he is an active revolutionary with a probability equal to p . The policemen's rule is therefore:

Rule P: randomly select an agent from the active citizens and active revolutionaries within vision radius v . If the randomly selected agent is a citizen, arrest him; if he is a revolutionary, kill him with a probability equal to p .

The same vision radius v is assumed for citizens, revolutionaries and policemen. Furthermore, parameters r and p can also be interpreted in terms of weapon precision or, more broadly, in terms of effectiveness in the military capacity of the conflicting parties. Once killed, revolutionaries and policemen are simply removed from the bidimensional space.

Finally, citizens who are not in jail, revolutionaries and policemen who are not killed can move in the lattice space to a random site without agents or in which there are only jailed citizens following this simple rule:

Rule M: within vision radius v , randomly move to an empty site or to a site in which there are only jailed citizens.

Table 1.1 presents the parameter values that are kept constant in all model simulations: the values assigned to the lognormal parameters (a, b) and the cost function parameter w_2 are selected in order to obtain a widespread distribution of hardship and opportunity costs on the $(0, 1)$ interval, avoiding concentration at the extremes of that interval; the other values are

Parameter	Description	Value
Citizen Density	Space occupied by citizens	70%
Revolutionary Density	Space occupied by revolutionaries	3%
Policeman Density	Space occupied by policemen	4%
Lattice Dimension	Dimensions of the bidimensional space	40x40
l	Government legitimacy	0.85
(a, b)	Lognormal parameters	(0.5, 0.5)
w_1	Arrest probability parameter	2.3
w_2	Cost function parameter	0.025
f	Citizens' activation threshold	0.1
v	Vision radius	7
j_{max}	Maximum number of periods in jail	30

Table 1.1: Parameter values fixed in all model simulations.

assigned according to those selected by Epstein (2002). The next section of the paper investigates the effects of the new parameters introduced by the present model, i.e. the military effectiveness of the two factions (p, r) and the revolutionaries' threshold n .

At the beginning of each model simulation, the random values y_i are drawn from the lognormal distribution and the different agents are randomly situated on the sites of the lattice. Then, an agent is selected at random. Under rule M, he moves to a random position within his vision, where he acts according to rule C if he is a citizen, rule R if he is a revolutionary or rule P if he is a policeman. This procedure is replicated until a given time or a specific condition (e.g. all revolutionaries or policemen are killed) is reached. The model was written using NetLogo (Wilensky, 1999), whereas the statistical analysis was performed using R (R Core Team, 2014).

1.3 Model Results

Three distinct outcomes can be identified by simulating this simple model: a successful revolution in which all policemen are killed by revolutionaries, leading to an overthrow of the central government; a failed revolution followed by a state of anarchy due to the large number of policemen killed; a completely failed revolution with only a few policemen killed, signifying a

return to the status quo after the uprising.

Figure 1.1 shows these possible outcomes with three simulations in which the random seed and the value of n ($n = 1.2$) are the same but the two precision parameters take different values: in particular, in the two upper graphs $p = 0.4$ and $r = 0.3$; in the middle pictures $p = 0.9$ and $r = 0.3$; finally, in the lower graphs $p = 0.9$ and $r = 0.1$. All three simulations start with a period of instability characterised by minor revolts where the poorest component of the population, made up of citizens with the greatest degree of grievance and the lowest opportunity cost, decides to rebel. However, these riots are too small, meaning that they do not degenerate into a revolution. This politically unstable pre-revolutionary period is a common feature of many historical revolutions: e.g. the strikes and workers' demonstrations in Russia (1917), Iran (1977-1978) and the Arab World (2011), motivated to a great extent by poor economic conditions such as low wages, high inflation (especially high food prices, as documented by Lagi, Bertrand and Bar-Yam, 2011), inequality, unemployment, as well as by a small degree of political legitimacy, due to the Russian Tsar's war defeat or the Shah's unpopular westernised costumes in the case of Iran.

Around time 30 a major riot occurs, and the revolutionaries' threshold rule is satisfied: this implies that revolutionaries become active and the rebellion, that started as a riot motivated by the poorest citizens' bad economic conditions, has now the features of a political revolution. The revolutionaries' threshold n therefore plays an important role because it determines the time at which revolutionaries will become active (in this specific simulation, $n = 1.2$). When revolutionaries become active, the citizens' estimated probability of arrest is lowered, creating a surge in the number of active citizens. Moreover, this effect is reinforced by the fact that revolutionaries start killing policemen, again lowering the probability of arrest. What happens next depends on the parameters that regulate the relative strength of the two factions.

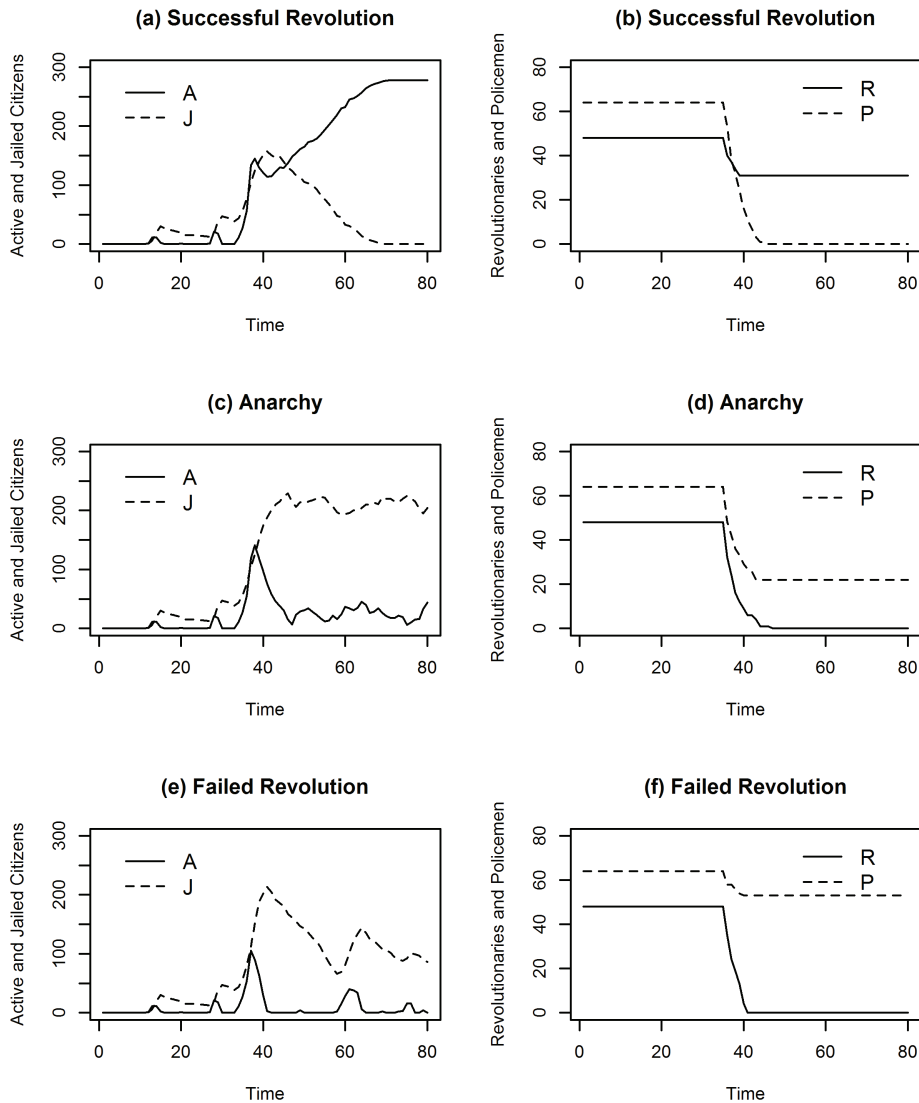


Figure 1.1: The three model outcomes. Time series graph for the different model scenarios: (a) time series of the number of active and jailed citizens in a successful revolution; (b) time series of the number of revolutionaries and policemen who have survived a successful revolution; (c) time series of the number of active and jailed citizens in an anarchic scenario; (d) time series of the number of revolutionaries and policemen who have survived an anarchic scenario; (e) time series of the number of active and jailed citizens in a failed revolution; (f) time series of the number of revolutionaries and policemen who have survived a failed revolution.

In the two upper graphs ($p = 0.4$ and $r = 0.3$), once revolutionaries have taken action, a large number of citizens become active, and policemen find more readily active citizens than revolutionaries: this explains why, following the surge, many citizens are arrested and only a few revolutionaries are killed. Hidden among active citizens, revolutionaries shoot policemen; when many are killed, the number of active citizens starts to increase again and, when all policemen have been killed, it reaches its maximum, i.e. all citizens with a degree of grievance exceeding the threshold become active: the revolution is complete and the government is overthrown. Political scientists (see Goldstone, 2001) have observed a common feature in all successful revolutions: they only occur when there is a link between mass mobilisation and the revolutionary movements that place themselves at the head of popular revolts, giving them organisation and coherence. This occurred with the Bolsheviks and the workers' riots in 1917 and with the Ayatollah Khomeini and the protests in the Iran's bazaars. The model is capable of capturing this link between popular spontaneous riots and organised action by revolutionaries. Examples of successful rebellions are represented by the three major historical revolutions in France (1789), Russia (1917) and Iran (1979), as well as by the recent uprisings in Tunisia (2011). In all these cases, the pre-revolutionary government is overthrown and a new order is established.

Conversely, in the middle graphs ($p = 0.9$ and $r = 0.3$), after the surge of active citizens, the armed conflict between revolutionaries and policemen is won by the latter. Nevertheless, a large number of policemen are killed and the revolution is followed by a period of major, never-ending turmoil: the huge reduction in the state's legal capacity, caused by the uprising, drives the country towards anarchy. A similar anarchic post-revolutionary situation usually follows a rebellion when the percentage of policemen killed exceeds 40% in the simulations. The anarchic outcome resembles the present civil war scenarios in Syria and Libya, where the 2011 insurrections com-

pletely destabilised these countries, reducing their government's capacity to rule.

Finally, in the lower graphs ($p = 0.9$ and $r = 0.1$), the difference in the military effectiveness of the two factions is too large, and only a few policemen are killed during the uprising (usually less than 40%). This means that, following a major rebellion, the situation is similar to that in the pre-revolutionary period: the status quo is maintained. Here the analogy is with the 2011 riots in Saudi Arabia and Bahrain, where opposition groups were very weak from a military perspective, and only a few police officers were killed in the street violence episodes.

In order to explore how the different outcomes of the model vary with the parameters associated with policemen's and revolutionaries' precision as well as with the threshold revolutionaries employ in their decision rule, the model was simulated for different values of these parameters: in particular, n takes values in the set $\{0.7, 0.8, 0.9, 1.0, 1.1, 1.2, 1.3, 1.4\}$, whereas the two precision parameters p and r assume values in $\{0.1, 0.2, \dots, 0.8, 0.9\}$ and $\{0.1, 0.2, 0.3, 0.4\}$, respectively. Finally, for each combination of these parameter values, the model is simulated 60 times, for a total of 17,280 simulations. Each simulation is halted after 300 time steps.

Figure 1.2 shows the average proportion of policemen killed in the simulations for different combinations of p and r (each mean is calculated employing 480 simulations, averaging over different values of n). The white and light grey regions represent the cases in which a return to the status quo arises after the uprising: the number of policemen killed is less than 40%. In fact, these areas correspond to a high value for policemen's precision and a low value for that of revolutionaries. As r increases or p decreases, the outcome of the simulations changes towards anarchy: these outcomes are represented by the darker grey areas, where the percentage of policemen killed is between 40% and 80%. Above a certain level for the two precision parameters, the situation changes from anarchy to successful revolution: the

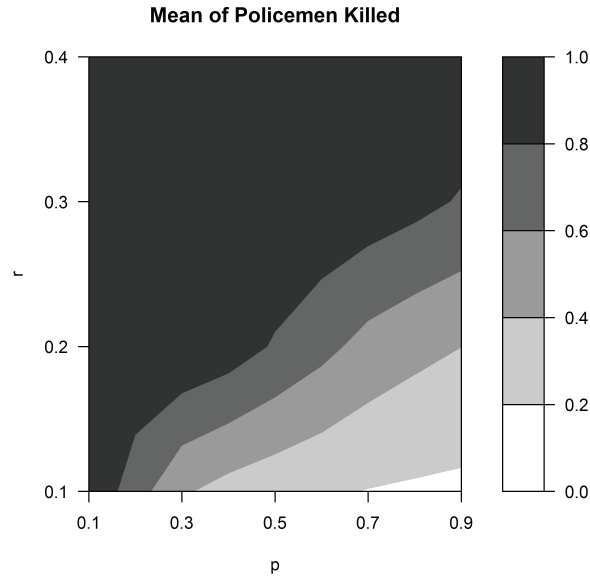


Figure 1.2: Average proportion of policemen killed for different values of the two precision parameters. For each combination of p and r , the average proportion of policemen killed is calculated employing 480 simulations.

regions for successful revolutions, where the average percentage of policemen killed exceeds 80%, are coloured black.

An important feature of the figure is that the white and light grey areas are well below the 45 degree line: this means that policemen need a very high level of precision compared to that of revolutionaries in order to win the armed conflict. This is due to the revolutionaries' strong advantage: in fact, they can hide among active citizens and attack when government forces are engaged in public order maintenance. This advantage results from the fact that policemen randomly draw one agent from the set of both active citizens and active revolutionaries within their vision radius (see rule P), and not from the set formed by revolutionaries only. This part of the model offers an incentive for revolutionaries to become active only when participation in spontaneous riots exceeds a minimum threshold. It also helps explain why, in the past, revolutionary movements occurred following strikes, protests and riots.

Figure 1.3 shows the same graph, albeit with the standard deviation of the proportion of policemen killed rather than the mean. First, it is

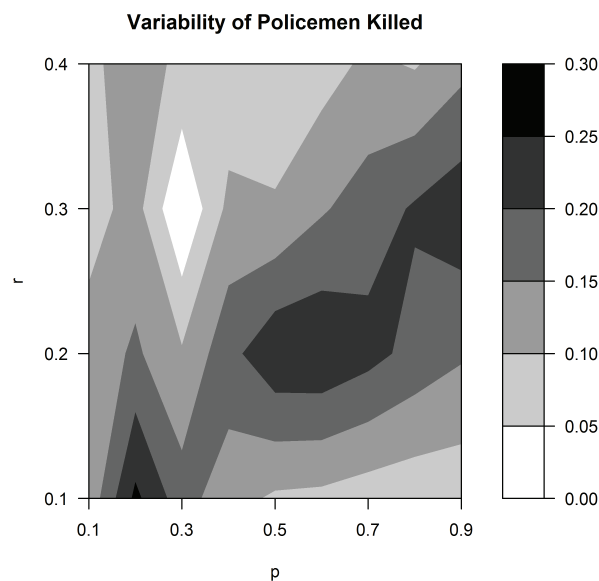


Figure 1.3: Variability of the proportion of policemen killed for different values of the two precision parameters. For each combination of p and r , the standard deviation of the proportion of policemen killed is calculated employing 480 simulations.

interesting to note that areas characterised by anarchy, in average terms, are also associated with a high variability of policemen killed (the dark grey and black areas). In contrast, the regions corresponding to a return to the status quo and the regions of successful revolutions display much lower levels of volatility: this means that, in these areas, the same outcome is often observed, while in the regions where anarchy, on average, is observed it is easier to observe diverse outcomes.

One of the main features shared by many revolutions in history is that they were not anticipated, neither by the government nor by the opposition. This pattern was first observed by Kuran (1989, 1991, 1995) in the dynamics of the French, Russian and Iranian revolutions and in the fall of communist regimes in Eastern Europe. A related interpretation was provided recently by Taleb and Treverton (2015), who point out that apparently stable regimes may be less well equipped to manage political instability than countries that are often affected by disorder and turmoil, which leads to their decline in the presence of significant and unanticipated shocks.

The model presented in this paper is able to replicate the unpredictable nature of revolutions. In fact, Figure 1.4 shows for three different values of n ($n = 0.8$, $n = 1.1$, $n = 1.4$) how many of the 2,160 simulations result in a revolution and the distribution of the time when rebellion occurs (the simulations employed have different values of p and r , but these parameters do not affect the timing of revolutions). For low and medium values of n , revolutionaries become active in every simulation and the time of activation is concentrated within 50 time steps. By increasing the value of the revolutionaries' threshold, a larger number of simulations do not result in a revolution, because the number of active citizens never reaches the level required for revolutionaries to become active, and the distribution of the time when rebellion occurs is more widespread. The revolutions generated by the model are therefore random events. In fact, it is impossible to anticipate if and when there will be a riot involving enough active citizens to activate the revolutionaries and generate an uprising. This behaviour of the model mimics real revolutionary events in which, as stressed by Goldstone (2011) in the context of the Arab Spring, opposition elites or defected military officers and most individuals who want to rebel against the government have an incentive to hide their true feelings until the crucial moment arises. It is also impossible to know which episode will lead to mass, rather than local, mobilisation.

1.4 Global Sensitivity Analysis

Using the same simulated data described in the previous section, several statistical models are estimated, in line with Saltelli *et al.* (2008), so as to help understand more rigorously how the three outcomes of the model depend on the two precision parameters and the revolutionaries' intervention threshold. In particular, the statistical analysis of the simulated data allows to estimate the impact of each model parameter controlling for the effects

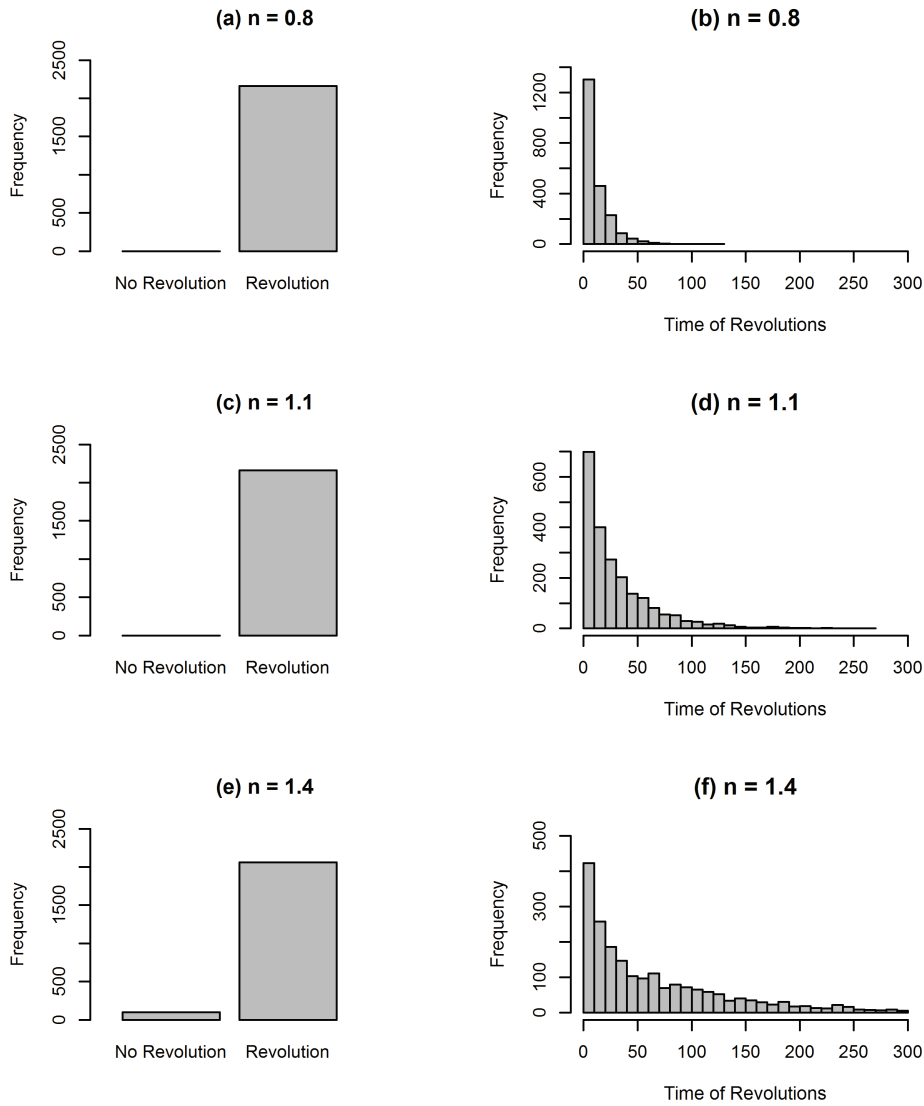


Figure 1.4: The unpredictability of revolutions. The graphs show how many simulations result in the occurrence of a revolution and the distribution of the time when rebellion occurs: (a) histogram of the number of revolutions that take place in 2,160 simulations for $n = 0.8$; (b) histogram of the time when revolutions occur for $n = 0.8$; (c) histogram of the number of revolutions that take place in 2,160 simulations for $n = 1.1$; (d) histogram of the time when revolutions occur for $n = 1.1$; (e) histogram of the number of revolutions that take place in 2,160 simulations for $n = 1.4$; (f) histogram of the time when revolutions occur for $n = 1.4$.

of the others.

In each simulation s a binomial distribution is assumed for the cumulative number of policemen killed z_s . The two parameters of this distribution are the number of policemen P and the probability of killing a policeman k , respectively. This last quantity, which can also be interpreted as a measure of the probability of a successful revolution, is assumed to be a function of the three most important parameters of the model, i.e. the precision of policemen p_s , the precision of revolutionaries r_s , the revolutionaries' activation threshold n_s :

$$z_s \sim \text{Binomial}(P, k(p_s, r_s, n_s)) \quad (1.7)$$

The model is estimated with different link functions for probability k , and the effect of n is included with a third-degree polynomial:

$$k(p_s, r_s, n_s) = g(\beta_0 + \beta_1 p_s + \beta_2 r_s + \beta_3 n_s + \beta_4 n_s^2 + \beta_5 n_s^3) \quad (1.8)$$

where $g(\cdot)$ can be the linear, logit, probit or complementary log-log link function.

The results are presented in Table 1.2: in the first column, the linear probability model (LPM) is estimated using the ordinary least squares estimator; in the other three columns, a different generalised linear model is estimated using the maximum likelihood estimator, assuming the link function of the logit, probit and complementary log-log model, respectively.

In all models, the two precision parameters have the expected signs: the policemen's precision has a significant and negative impact on the probability of killing a policeman because the higher the precision of governmental forces, the larger the number of revolutionaries killed and, consequently, the lower the effectiveness of revolutionaries in killing policemen; on the other hand, as expected, the revolutionaries' precision has a significant and

	(1)	(2)	(3)	(4)
	LPM	Logit	Probit	CLogLog
p	-0.498*** (0.006)	-4.969*** (0.014)	-2.740*** (0.008)	-2.438*** (0.007)
r	2.015*** (0.014)	20.120*** (0.044)	10.868*** (0.022)	9.154*** (0.020)
n	-0.079 (0.582)	-0.854 (1.145)	-1.917*** (0.641)	-2.722*** (0.601)
n^2	0.381 (0.572)	3.950*** (1.116)	3.870*** (0.625)	5.093*** (0.585)
n^3	-0.211 (0.183)	-2.181*** (0.354)	-1.846*** (0.198)	-2.440*** (0.185)
Constant	0.432** (0.193)	-0.940** (0.382)	-0.047 (0.214)	-0.118 (0.200)
Observations	17,280	17,280	17,280	17,280
R^2 /pseudo- R^2	0.623	0.692	0.685	0.656

Table 1.2: Estimates of the statistical models. Column 1: linear probability model estimated with ordinary least squares estimator, standard errors corrected for heteroskedasticity. Column 2: logit model estimated with the maximum likelihood estimator. Column 3: probit model estimated with the maximum likelihood estimator. Column 4: complementary log-log model estimated with the maximum likelihood estimator. (***) significant at 1%, ** significant at 5%, * significant at 10%)

positive effect on the probability of killing a policeman.

In order to analyse the effect of the revolutionaries' threshold n on the probability of killing a policeman, function $k(0.9, 0.3, n)$ is plotted in Figure 1.5 ($p = 0.9$ and $r = 0.3$ are plausible values for the two precision parameters) for the linear, logit, probit and complementary log-log model. In all specifications, it is evident that the probability of killing a policeman slightly increases in n up to a given value; then, the probability decreases markedly if n increases. A third-degree polynomial is preferred to a second-degree one because it allows this asymmetry to be captured. The intuition behind this shape is the following: for a revolutionary organisation, it is not optimal to start a revolution too early, when popular riots are small-scaled (small value of n), because it would easily come under fire from policemen. At the same time, however, revolutions may not occur if the revolutionary organisation waits too long (high value of n). According to these estimates,

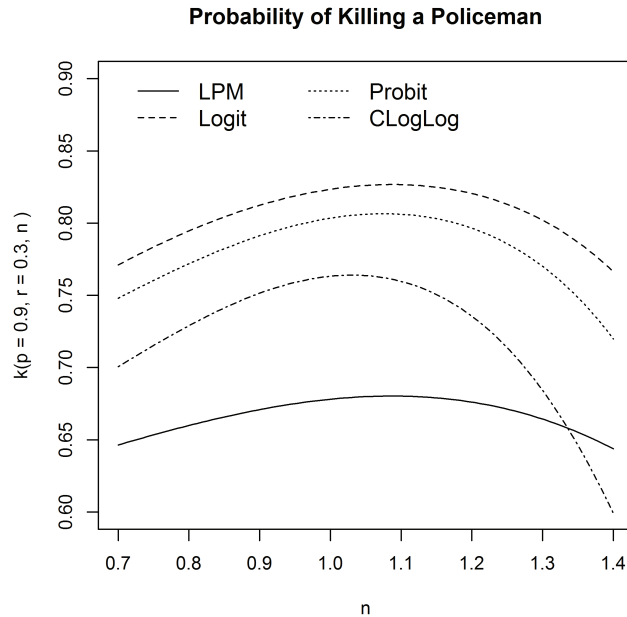


Figure 1.5: Probability of killing a policeman as a function of the revolutionaries' threshold. Function $k(0.9, 0.3, n)$ is plotted for the linear, logit, probit and complementary log-log model. .

if the revolutionary organisation's objective is to maximise the probability of a successful revolution, the optimal behaviour is to choose n in $[1.0, 1.1]$, which suggests starting the uprising when the number of active agents is equal to that of governmental forces or exceeds it by about 10%.

1.5 Stationarity and Ergodicity

In this section the emerging outcomes of the model are analysed with respect to the categories of stationarity and ergodicity (Grazzini and Richiardi, 2015). A model or, in general, a data generator process is said to be stationary if it converges to an equilibrium, while ergodicity tells whether such equilibrium is unique. Stationarity is a necessary but not a sufficient condition for ergodicity: in fact, the latter implies that convergence to the equilibrium state is guaranteed for every possible realization of the process, i.e. for every random seed.

In the present model, these two properties strongly depend on the values

of the precision parameters p and r . Figure 1.6a shows the time series of the number of active citizens in 100 simulations performed with $p = 0.4$ and $r = 0.3$. Each series stabilises on a constant value after the uprising which is equal to the number of citizens whose grievance is higher than the participation threshold. As a consequence, it is possible to conclude that each process is stationary. Moreover, since in every series the outcome observed is always a successful revolution and assuming that the number of simulations is sufficiently high and representative, we can also conclude that the process is ergodic.

A similar conclusion on the stationary and ergodic features of the model equilibrium can be derived in Panel 1.6b, in which $p = 0.9$ and $r = 0.1$: all the series are characterised by random peaks of active citizens, both before and after the rebellion. These outcomes correspond to the return to the status quo after the turmoil.

Results change completely in the last picture of Figure 1.6, where $p = 0.9$ and $r = 0.3$. In fact, in this scenario it is quite easy to detect the existence of three types of dynamics: some series are converging to the successful revolution outcome, as happened in Panel 1.6a; in other realizations of the process, the protests are completely suppressed and a pattern similar to Figure 1.6b is detected; finally, in some other cases, we observe the emergence of the intermediate outcome, labelled anarchy above, in which policemen are not able to reduce the level of protests after the uprising. This multiplicity of equilibria in correspondence to the same values of the model parameters, which ultimately depends only on the initial random seeds, is the typical expression of a non-ergodic behaviour.³

³It is worth stressing that the focus of this analysis is on the stationarity and ergodicity of the model with respect to the three outcomes (successful revolution, anarchy, and return to the status quo). Obviously, if the attention is strictly devoted to the number of active citizens, the model always displays a non-ergodic behaviour (detected by the formal test proposed by Grazzini, 2012) because the number of active citizens at the end of each run depends on the realization of the income process at the beginning of the simulation.

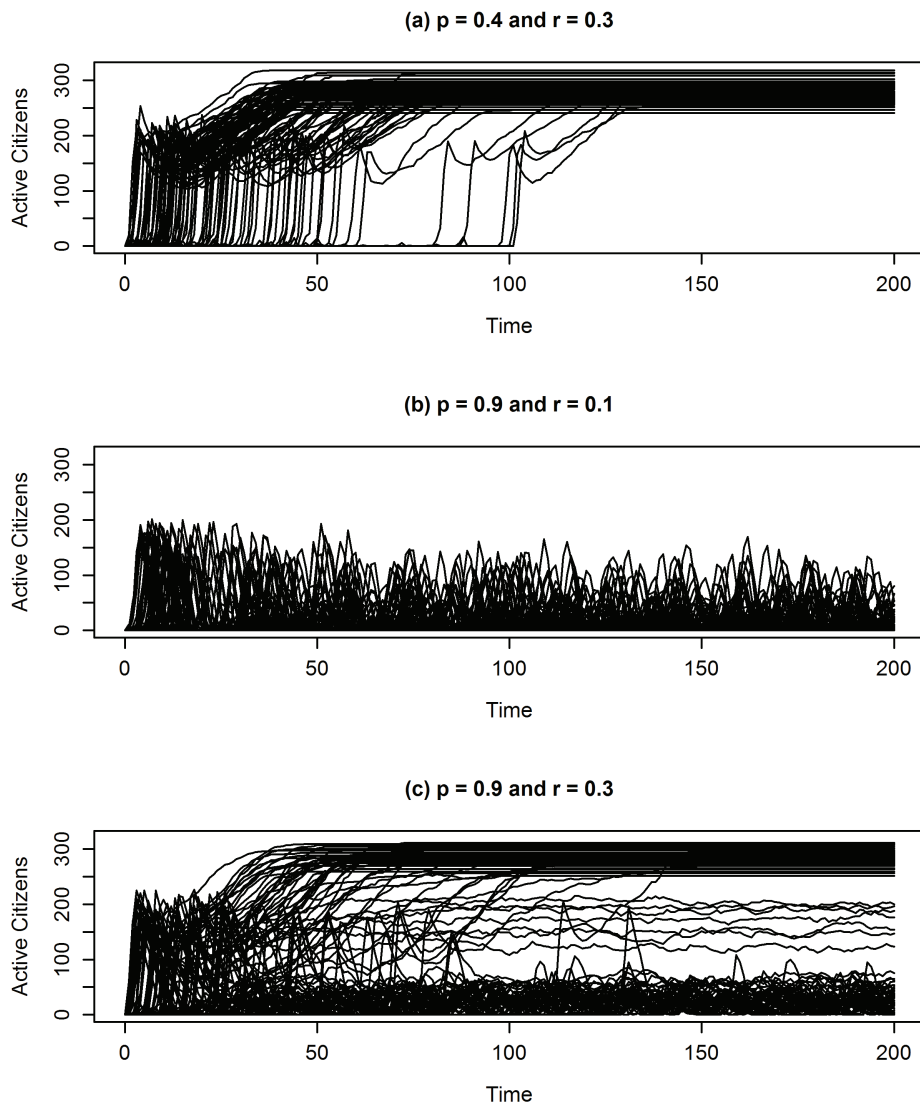


Figure 1.6: Discussion of the stationary and ergodic properties of the model for different values of the two precision parameters: (a) $p = 0.4$ and $r = 0.3$; (b) $p = 0.9$ and $r = 0.1$; (c) $p = 0.9$ and $r = 0.3$.

1.6 Discussion

Although the agent-based model presented in this paper is simple and makes no claim of incorporating all of the complex aspects involved in historical revolutions,⁴ it nevertheless captures several relevant stylised facts that are common to most revolutionary episodes in the real world.

The most important of these facts is represented by the multiplicity of different scenarios that can arise from a rebellion, i.e. a successful revolution, an anarchic scenario and the return to the status quo. The relevance of this last aspect can be understood by considering recent experience in the Arab Spring, where many rebellions, that seemed to start in 2011 in a similar way, resulted in completely different political outcomes.

Moreover, this model generates a plausible dynamics, coherent with major political revolutions, that can be summarised as follows: a pre-revolutionary period characterised by spontaneous riots motivated mainly by poor economic conditions and social inequality, followed by a proper revolutionary rebellion where organised and politically oriented elements mobilise popular masses against the central authority. This dynamics mimics the sequence of events of most historical revolutions, and is consistent with the political science literature, which stresses the role played by revolutionary elites in the organisation of successful revolutions.

Furthermore, this paper examines the trade-off that revolutionaries face in deciding when to become active: if they start an uprising too early, when popular riots are minor, they will directly come under fire from policemen; on the other hand, if they wait too long, the revolution may not occur at all. If the revolutionary organisation's objective is to maximise the probability of a successful revolution, the optimal threshold should balance these two

⁴A debatable assumption of the model is that the size of the revolutionary group is fixed and revolutionaries cannot be joined by new adepts from the civil population. However, without this assumption, the likelihood of a successful revolution would be much increased, reducing the probability of the other two scenarios. Consequently, this would compromise the richness of the model predictions about the outcomes of a revolution.

opposite forces, and riots that do not exceed this minimum level of rebels will not degenerate into revolutions.

This paper also stresses the random nature of revolutions, pointing out that rebellions arise from interactions between many agents, determining their unpredictability: it is impossible to anticipate with certainty when and which riot will degenerate into a revolution. This consideration implies that similar countries, in terms of institutions and political systems, may experience revolutionary events at different points in time, or that some may not experience revolutions at all.

A policy implication that can be derived from the model is as follows. Let us suppose that a foreign state wants to intervene in another state to support a revolutionary group by providing more effective weapons in order to overthrow the existing government. In the framework of the model, this is translated into an increase in the revolutionaries' effectiveness captured by parameter r . It is also assumed that, without external intervention, the initial configuration of precision parameters would have led to a rebellion followed by a return to the status quo. If the increase in revolutionaries' precision is not sufficiently large, as shown in the graph in Figure 1.2, the political situation may degenerate from a relatively stable situation, the return to the status quo (the white and light grey areas in the figure), to an unstable one, characterised by a rebellion resulting in anarchy (the darker grey area in the figure). This implies that the foreign government should provide enough support in order to deliver a successful revolution as the final result (the black area in the figure). Mistakes in the determination of this support may precipitate a country towards a state of persistent turmoil and civil war.

In conclusion, it is worth stressing that having real data, on a daily or monthly basis, on the number of citizens who decide to rebel against a government and on the participation of revolutionaries in these events, it would be possible to calibrate the model using such data and to identify the most

probable outcome in the case of future revolutionary episodes. Therefore, despite this falls outside the limits of the present analysis, the proposed approach can be useful to derive important policy recommendations.

Chapter 2

Evaluating the Effect of Gun Availability on Homicides through an Agent-Based Model

Abstract

The aim of this chapter is the evaluation of the effects of gun availability on firearm-related homicides in an agent-based framework. Behind this relationship there is a likely trade-off: on the one hand, a diffused gun ownership can protect victims against the attacks of violent individuals; on the other hand, a higher diffusion of weapons increases the probability that a violent individual can obtain a gun. The analysis of this paper reveals that, with a high number of police officers relative to the space and the number of citizens, it is possible to minimise the number of homicides either with a complete ban of weapons or with a capillary diffusion of guns. Conversely, when the number of police officers is relatively low, only a policy that reduces gun availability close to zero minimises the firearm-related deaths. Moreover, a greater presence of policemen generates a transition from a private kind of self-defense to a public one. Furthermore, the model discusses the impact of some social variables included in the model on the

number of killings. Finally, the analysis of simulated data reveals that the variability of homicides closely tracks the behaviour of their average value.

2.1 Introduction

The aim of this paper is the evaluation of the effects of gun availability on firearm-related homicides in an agent-based framework. The topic of gun violence has received an increasingly greater attention in the public debate, especially in the United States, and in the scientific literature because its incidence can be compared to that of diseases of major public health concern (Hemenway and Miller, 2000; Hemenway, 2006). Moreover, the frequency of gun-related homicides has been associated with many social, economic and political factors (Kennedy *et al.*, 1998; McCall *et al.*, 2008): for instance, one of the most crucial variables that should affect homicides is represented by the degree of diffusion of guns in the population, which depends on the legislation and the controls adopted in each country.

However, the possible presence and sign of the effects of gun availability on firearm-related homicides have been debated (Kleck and Gertz, 1995; Jacobs, 2002; Lott, 2010). In fact, behind the relationship between weapon availability and homicide rates there is a likely trade-off: on the one hand, a diffused gun ownership can protect victims against the attacks of violent individuals; on the other hand, a higher diffusion of weapons increases the probability that a violent individual can obtain a gun.

Several empirical studies have investigated the relationship between homicides and having a gun in the home (Kellermann *et al.*, 1993; Wiebe, 2003), purchasing a gun (Cummings *et al.*, 1997; Grassel *et al.*, 2003), owning a gun (Kleck and Hogan, 1999), or possessing a gun in proximity of shootings (Branas *et al.*, 2009). However the results of these studies can only be interpreted as correlations without any claim of causal effects: in fact, these works do not address the endogeneity issue due to the possible re-

verse causality between gun possession and gun assault. The limitations of the existing data on gun possession and homicides suggest the adoption of different approaches.

A paper that explores in depth the trade-off behind the relationship between gun availability and firearm-related homicides in a mathematical framework is represented by the work of Wodarz and Komarova (2013): the authors find that in principle two possible scenarios can minimise the death rate, i.e. a ban of private weapon possession or a complete liberalization of gun ownership. Which of these two policies really minimises the number of homicides depends on some important parameters, including the fraction of offenders that illegally possesses a gun, the degree of protection provided by gun ownership and the fraction of the population who owns a gun and carries it when attacked.

The present paper examines a similar trade-off but using a computational agent-based model. This methodology represents a more powerful framework to analyse problems in which the time and space dimensions as well as the interactions among different players, like victims and offenders, play a fundamental role because these features are easily implementable within the agent-based approach.

To the best of our knowledge, there is only another paper written by Hayes and Hayes (2014) that uses an agent-based model to study a similar phenomenon, i.e. mass shootings. However, the aim of that work is the evaluation of a specific policy intervention, namely an assault weapons and high-capacity magazines bill, and the focus of the paper is therefore on technical variables, like the accuracy, the magazine capacity and the rate of fire of weapons, and on their impact on mass shootings.

Conversely, the present paper is more concentrated on other factors, like the presence of police officers, the effect of a lower lifetime combined with higher birth rates, the incidence of a more violent society, and on the effects of these variables on the trade-off described above.

The analysis reveals that, in the presence of many police officers and a diffused control of the territory, it is possible to minimise the number of homicides either with a complete ban of weapons or with a capillary diffusion of guns. On the contrary, with a low number of police officers relative to the space and the number of citizens, only a gun availability close to zero minimises the firearm-related deaths. Moreover, the greater presence of policemen generates a transition from a private kind of self-defense to a public one. The model also predicts that an increase of natural mortality, associated also with high birth rates, and a more violent society can have a greater impact on homicides than more precise weapons.

The paper also examines the variability of homicides committed for different values of the model parameters: results indicate that the behaviour of the variability of killings closely tracks the dynamics of their average value, meaning that the same value of gun availability maximises both the average number and the standard deviation of homicides.

Finally, the model is slightly modified in order to consider the effects of the spatial concentration of agents in specific neighbourhoods and more sophisticated forms of interaction between violent and nonviolent citizens.

The rest of the chapter is organised as follows: next section describes in detail the theoretical framework and the adopted agent-based model, focusing on the description of the different agents and their simple behavioural rules; Section 2.3 presents the experiments performed and analyses the main results; finally, Section 2.4 concludes.

2.2 The Model

This section of the chapter firstly presents a theoretical framework, similar to the one of Wodarz and Komarova (2013), in which the gun diffusion trade-off is formally presented and discussed. The adopted agent-based model immediately follows as a natural extension of this framework. This modeling

approach is motivated by the capability to enrich the analytical analysis by explicitly considering important factors, like the interactions between victims and offenders or between killers and policemen, and studying the impact of scale and spatial effects on the evolution of the system.

2.2.1 A Theoretical Framework

It is assumed that a population consists of C citizens and P policemen. In this population there is a percentage v of violent individuals and a fraction α of armed individuals: these two characteristics are independently distributed in the population. These two parameters significantly affect the number of killers K through the following relationship:

$$K = \phi(\alpha)\alpha vC \quad (2.1)$$

where αvC is the number of individuals that are both violent and armed (potential killers), whereas $\phi(\alpha)$ represents the fraction of potential killers that really decide to commit homicide. This last quantity is negatively affected by the deterrence effect represented by the number of policemen P and by the number of citizens carrying a gun αC , because each potential killer takes into account the possible presence of policemen or armed individuals who can defend themselves before selecting a victim. The chosen expression for $\phi(\alpha)$ is therefore:

$$\phi(\alpha) = \exp(-\beta P - \gamma \alpha C) \quad (2.2)$$

in which β and γ are two positive coefficients. The number of homicides H is simply a function of the number of killers K :

$$H = \psi(K) \quad (2.3)$$

where $\psi(\cdot)$ is a strictly increasing function. Finally, the government chooses the optimal gun control policy α in order to minimise the number of homicides or, equivalently, the number of killers:

$$\min_{\alpha} \{ \exp(-\beta P - \gamma \alpha C) \alpha v C \} \quad (2.4)$$

The first order condition (FOC) of the above minimisation problem is given by:

$$\frac{\partial K}{\partial \alpha} = -\phi(\alpha) \gamma \alpha v C^2 + \phi(\alpha) v C \quad (2.5)$$

The FOC makes explicit the trade-off behind gun diffusion: the first term in the right-hand side represents the negative effect on the number of killers due to the increase of the number of armed citizens that can defend themselves from the attacks of violent individuals; the second term captures the positive effect given by the easier access to weapons for criminals. The deterrence effect prevails on the diffusion effect if the following inequality holds:

$$\gamma \alpha C > 1 \quad (2.6)$$

The inequality is more likely satisfied if the fraction of killers $\phi(\alpha)$ is more sensible to the number of armed citizens (high value of γ) or if there are more armed individuals αC . Furthermore, the FOC implies that K , as a function of α , has a hump-shaped profile in which the maximum number of killers is obtained for a value of α equal to:

$$\alpha^M = \frac{1}{\gamma C} \quad (2.7)$$

For values of $\alpha < \alpha^M$, a higher diffusion of weapons increases the number of killers because the diffusion effect prevails; on the other hand, beyond α^M the deterrence effect is stronger and K is a decreasing function of α . For this reason there are two minima, whose coordinates are $(\alpha_1^m = 0, K_1^m = 0)$ and

($\alpha_2^m = 1, K_2^m = \phi(1)vC > 0$): therefore, for the problem specified above, the optimal policy is a complete ban of weapons.

However, in some cases, a value of α equal to zero might be unfeasible: for instance, in the presence of an illegal market of weapons the government is not able to enforce a complete ban of guns. Under these circumstances, a widespread diffusion of guns may be optimal. Formally, if $\underline{\alpha}$ denotes the minimum possible value of α , the scenario in which $\alpha = 1$ is the optimal policy as long as:

$$\exp(\gamma(1 - \underline{\alpha})C) \underline{\alpha} > 1 \quad (2.8)$$

whose likelihood, as inequality (2.6), positively depends on both the sensibility to the presence of armed citizens γ and to the difference in the number of armed individuals $(1 - \underline{\alpha})C$ in the two cases.

The rest of the chapter will enrich this analysis using an agent-based model that considerably extends the present framework.

2.2.2 The Agent-Based Extension

The agent-based model presented in this subsection consists of C citizens interacting over time in a bidimensional torus space.¹ As in the previously described theoretical framework, each citizen has an exogenous probability v of being violent and an exogenous probability α of being armed: the former parameter indicates the rate of violence in the society, while the latter measures the degree of gun availability. At each time step citizens can move to a random site within their vision radius, where they act according to some simple behavioural rules: in particular, citizens that are both violent and armed decide whether or not to kill other citizens, whereas armed citizens that are nonviolent can react when attacked by violent individuals protecting themselves and killing violent agents. In the model there are

¹It is possible to interpret this bidimensional space as an urban environment, like a town or a city.

also P policemen that have being tasked to suppress the killers. The rules and the behaviours of each type of agent will be described in detail in this subsection.

Individuals that are both violent and armed decide to become active killers or remain quiet using a threshold-based rule involving the number of policemen and the number of potentially armed citizens in their neighbourhood, i.e. inside the space within their vision radius, and they become killers if the number of policemen and armed citizens is low. According to this idea, citizen i , if armed and violent, counts the number of policemen P_i and the expected number of potentially armed citizens αC_i inside his vision radius;² then, he becomes an active killer if and only if the following inequality holds:

$$P_i + \alpha C_i < \tau \quad (2.9)$$

in which τ represents the maximum number of opponents that the killer is willing to face. If citizen i decides to be a killer, he randomly chooses a citizen as a potential victim inside his neighbourhood, and kills him with a probability equal to π .³ The idea of employing a threshold-based model was introduced in Granovetter's (1978) fundamental paper and it is widely used in the agent-based literature, such as in the civil violence model of Epstein (2002). It is worth stressing that violent and armed citizens are endowed with some degree of rationality: in fact, according to inequality (2.9), they take into account the risk of meeting policemen and armed citizens before becoming active killers.

Conversely, armed citizens who are not violent can defend themselves by killing, with the same probability π , a killer picked at random in their

²It is assumed that the theoretical probability that a citizens is armed in the population, i.e. α , is common knowledge, while the fact that a single citizen is effectively armed is private information. Therefore, killers estimate the expected number of potentially armed citizens in their neighbourhood as the product between the number of citizens C_i inside their vision radius multiplied by the probability that each of them is armed α .

³A complementary interpretation is that homicides can be the result of the interactions and relationships between a violent individual and his peers in the neighbourhood.

vision radius. Moreover, the elimination of killers is the main task of the other type of agent in the model, i.e. the police officers: they have the duty to inspect the positions in their neighbourhood and suppress a randomly selected killer with the same probability π . Therefore, the only difference between policemen and nonviolent and armed citizens is that the former agents cannot be selected as potential victims by killers and, hence, they never die.

As in the civil violence model of Epstein's (2002) paper, each citizen is endowed with a maximum number of periods of life, drawn from a discrete uniform distribution on the $(0, L_{max})$ interval: age is increased by one unit at the end of each time step and citizens die once their maximum age is reached. When citizens die, either by natural or violent causes, they are replaced by an exact number of new agents, so that the population of citizens is constant over time.

The model is implemented in NetLogo (Wilensky, 1999). The user can choose the values of the model parameters, agents are randomly located in the bidimensional torus space, and each citizen randomly receives the maximum number of life periods and the two characteristics (i.e., violent/nonviolent and armed/unarmed). In every time period the simulation evolves through the following steps:

1. an agent is randomly selected;
2. the chosen agent moves to a random site within his vision radius;
3. the selected agent behaves according to the specific rules of his type:
 - (a) if he is a violent and armed citizen, he decides whether or not to become a killer following inequality (2.9): if he becomes a killer, he randomly chooses a citizen inside his vision radius and he kills the victim with the given probability. Otherwise, he remains quiet;

- (b) if he is a nonviolent and armed citizen, he randomly chooses a killer inside his vision radius and he kills him with the given probability;
- (c) if he is a police officer, he randomly chooses a killer inside his vision radius and he kills him with the given probability;
- (d) unarmed citizens, both violent and nonviolent, do not perform specific tasks.

These simple rules are replicated for all agents. Once all agents have performed their tasks, the age is increased by one unit, and citizens who reach their maximum age die. All agents that die due to natural or violent death are removed from the bidimensional space. Then, a new time period begins, new citizens replace the dead ones and the procedure is performed again until the user quits the simulation or a specified time is reached. At the end of each simulation, the cumulative number of homicides committed by killers and the number of killings performed by police officers or by self-defense are recorded.

2.3 Results

The previous model is simulated for different values of the parameters with the aim of analysing how homicides depend on the degree of gun availability and testing whether this relationship is robust to alternative specifications of the model and to different values of its parameters.

In particular, Table 2.1 summarises the main experiments performed: the first experiment is the baseline scenario, in which the bidimensional space has dimensions equal to 16x16 patches, the precision of weapons π is 0.6, and each of the 700 citizens has a maximum life drawn from a discrete uniform distribution on the (0, 100) interval and a probability of being violent v equal to 0.05; in the second experiment, the space is enlarged (32x32

Experiment	Name	Space	π	L_{max}	ν	Simulations
1	Baseline	16x16	0.6	100	0.05	1,040
2	Larger Space	32x32	0.6	100	0.05	1,040
3	Higher Precision	16x16	0.8	100	0.05	1,040
4	Higher Mortality	16x16	0.6	50	0.05	1,040
5	More Violence	16x16	0.6	100	0.10	1,040

Table 2.1: Values chosen for the main parameters of the model in the five experiments performed. The baseline scenario is represented by experiment 1. The changes made with respect to the values of the parameters in the first scenario are highlighted in bold. In all experiments the number of citizens C is equal to 700, the killers’ threshold τ is equal to 2, the length of the vision radius is 1.5 patches for each agent, while α and P take different values in the simulations performed.

patches), keeping fixed the values of the other parameters; in the third scenario the precision is higher and equal to 0.8, while in the fourth one the maximum life L_{max} is reduced to 50, *coeteris paribus*; finally, in the last experiment the percentage of violent citizens is equal to 10%.

In all simulations, the number of citizens C is 700, the killers’ threshold τ is equal to 2, the length of the vision radius is 1.5 patches for each agent, and the halting time is 500 time steps. Moreover, in order to analyse the behaviour of the model for different values of the gun availability parameter α and for different numbers of police officers P , in every scenario these two parameters take values in the following sets: $\{0.01, 0.05, 0.10, 0.20, \dots, 0.80, 0.90, 0.95, 0.99\}$ and $\{50, 100, 200, 300\}$, respectively. For each combination of parameter values, the model is simulated 20 times: this implies that each experiment consists of 1,040 simulations.

The values of the parameters in the baseline scenario as well as in the alternative settings are chosen in order to ease interpretation and explore a variety of possible parametric constellations.

In every scenario, the number of homicides performed by killers is recorded, together with the number of killings made by armed and nonviolent citizens for self-defense or by police officers: these variables will be the objective of the following analysis.

2.3.1 Homicides Committed and Gun Availability

In this subsection, the dependence of the number of homicides committed on gun availability is studied. In particular, the results for the first scenario are displayed in Figure 2.1. This picture shows on the horizontal axis different values for the gun availability parameter, whereas on the vertical axis the total number of homicides performed by killers is reported. Each curve is a non-parametric estimate of the relationship between homicides and gun availability using the simulated data and corresponds to a different number of police officers. All of them exhibit a hump-shaped profile (similar to the graph in Wodarz and Komarova, 2013) and the minimum number of killed agents is reached when α is close to zero, i.e. when weapons are banned and it is not possible to obtain them in any legal or illegal way. By increasing the value of gun availability beyond zero, the number of homicides raises because the likelihood that a violent citizen is armed increases too. However, this profile reaches a maximum and then declines: the reason is that nonviolent citizens are also more likely to have a gun and, therefore, they can shoot killers for self-defense; at the same time, the higher likelihood of meeting armed citizens discourages the activation of killers through inequality (2.9). These reasons explain why the peak in the number of homicides is reached in correspondence to the same value of α for which the number of active killers is maximised.

It is worth noting that, when the number of police officers is high, it is possible to reduce the number of homicides to a value comparable to the situation in which α is close to zero even when α assumes a much higher value: this happens because the combination of a high number of policemen and armed citizens lowers the probability that the killers' threshold rule is satisfied. On the other hand, when there are few police officers, even a value of α close to one is not able to reduce the number of homicides to zero.

This last effect is more evident considering the curves of the experiment

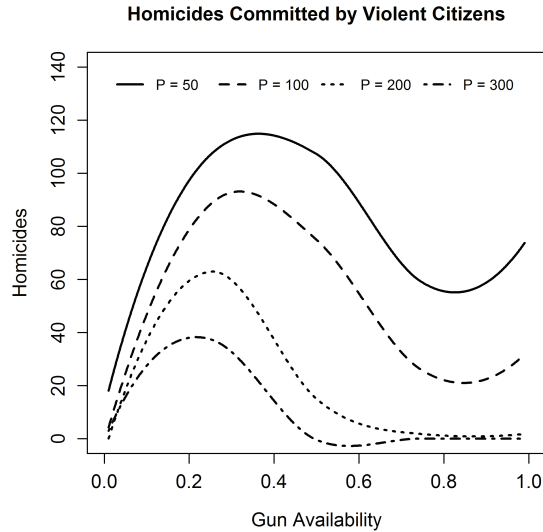


Figure 2.1: Number of homicides committed for different values of gun availability and different numbers of police officers in the baseline scenario (experiment 1).

with a larger bidimensional space, plotted in Figure 2.2. In this scenario, the number of homicides is an increasing function of the percentage of gun diffusion α : this means that, when α increases, the greater presence of potential killers overcomes the deterrence effect of a higher number of armed and nonviolent citizens. The weakness of the deterrence effect is motivated by the low number of policemen compared to the new dimensions of the space.

It is interesting to notice that in both experiments the marginal effect of adding new police officers is a decreasing function of the number of policemen: in fact, the increase of police officers from 100 to 200 has a much larger effect on the number of committed homicides than the increase from 200 to 300. This feature of the police repression technology is also present in Hayes and Hayes (2014).

2.3.2 Police versus Self-Defense

It is reasonable to think that a lower presence of police officers should be associated with an increase in the relevance of self-defense, because citizens

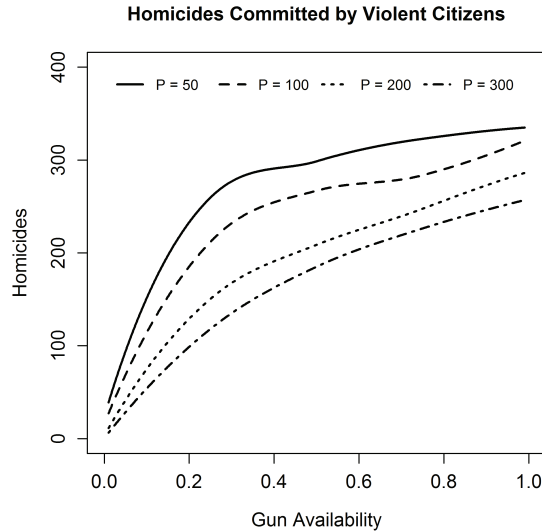


Figure 2.2: Number of homicides committed for different values of gun availability and different numbers of police officers in the larger space scenario (experiment 2).

are forced to protect themselves with their own weapons. It is possible to test this hypothesis using the simulated data.

Considering again the baseline scenario, the difference between the number of violent and armed citizens killed by police and those killed for self-defense is analysed in Figure 2.3 according to different values of the gun availability parameter and different numbers of police officers. This picture reveals that when the number of policemen is low (50 or 100) there is a prevalence of self-defense killings for almost all values of the gun availability parameter: the minimum of the difference of killings coincides with the intermediate value of α for which the activation of killers is maximised. On the other hand, for a high number of police officers (for instance, 300) there is a prevalence of killings caused by police intervention. Therefore, the greater presence of police officers leads to a transition from a private to a public kind of defense.

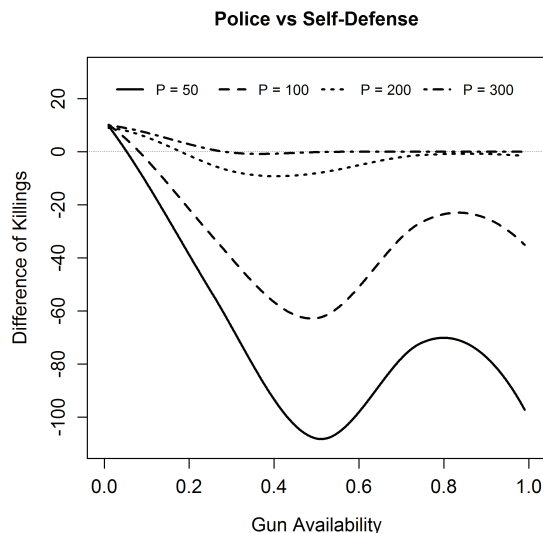


Figure 2.3: Difference between killings performed by police officers and those committed for self-defense in correspondence to different values of gun availability and different numbers of police officers in the baseline scenario (experiment 1).

2.3.3 The Other Factors

This subsection explores the dependence of the homicides committed on the other variables of the model. In particular, the effects of a higher precision of weapons, a lower lifetime and a more violent society on the number of homicides are compared to the baseline scenario in Figure 2.4. The picture shows that all these factors increase the number of killings performed by violent citizens.

In particular, the effect of the increase of gun precision is positive because killers' guns are more lethal. However, this effect is the smallest one because police officers and armed nonviolent citizens have more precise weapons too.

The positive effect of the lifetime reduction on the number of homicides committed can be understood considering that a higher mortality is compensated by the birth of new agents in this model. Since at every time step a higher number of citizens is generated, keeping fix the probability that each of them is violent and armed, the number of potential killers increases on average.⁴

⁴In order to understand if this feature assumed in the model is realistic, i.e. the

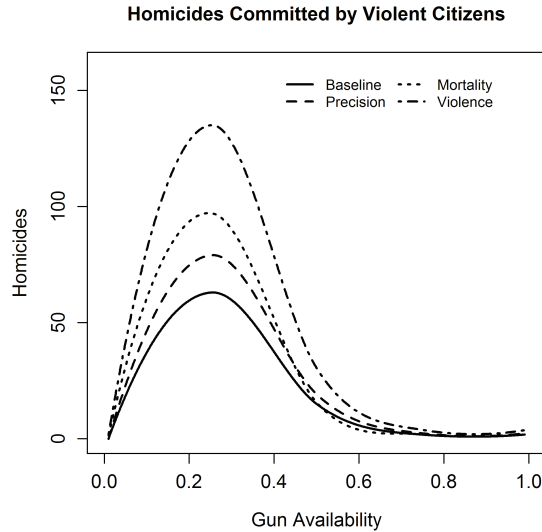


Figure 2.4: Number of homicides committed for different values of gun availability and different numbers of police officers in the baseline, high precision, low lifetime and high violence scenarios (experiments 1, 3, 4, 5).

On the other hand, the highest effect on the number of homicides committed is obtained in correspondence to an increase in the percentage of violent agents, meaning that a violent society is the principal cause of crimes and disorders, at least according to the model.

It is worth noting that these effects are amplified for the intermediate values of α in which the activation of violent agents is maximised, whereas they are reduced significantly in correspondence of both low and high values of α , i.e. when there are few weapons or the maximum deterrence effect of gun availability is reached.

2.3.4 Variability of Homicides

With the same simulated data it is also possible to study the variability of homicides, by calculating the standard deviation of killings for different

positive relationship between a lower lifetime and a higher number of agents generated in each period, we have to consider that poor societies, characterised by a low life expectancy, often tend to present high birth rates too. Therefore, the prediction of the model about a positive correlation between mortality and violence may be plausible for those societies. Certainly, this implication of the model must be considered with caution because we are not controlling for the other socio-economic factors which are likely to have an impact on the number of homicides.

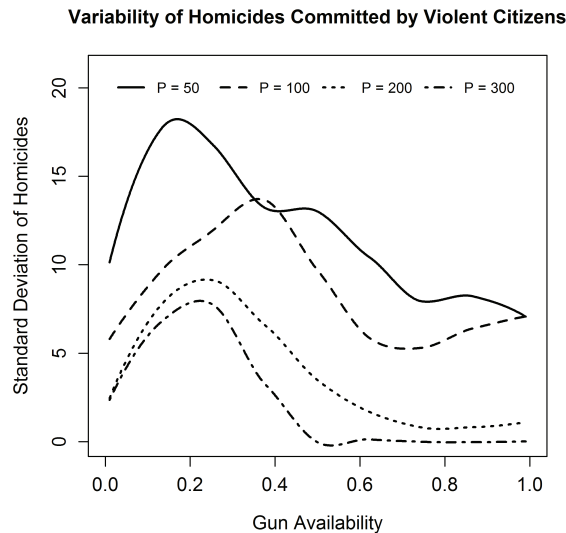


Figure 2.5: Variability of homicides committed for different values of gun availability and different numbers of police officers in the baseline scenario (experiment 1).

values of the model parameters.

In particular, the curves in Figure 2.5 represent a non-parametric fit of the standard deviation of homicides in correspondence to different values of gun availability and different presence of police officers, using the data of the first experiment. By comparing this picture with Figure 2.1, we can see that the maximum in the variability is reached in proximity of the peak in the number of killings: in other words, roughly the same value of gun availability α maximises both the number of homicides and their variability. From Figure 2.5, it is also evident that an increase in the presence of policemen leads to a reduction in the variability of homicides, and not only to a fall in the number of homicides, as was clear in Figure 2.1. Moreover, the same decreasing marginal effects of the police presence are observable in this picture as they were in Figure 2.1.

Figure 2.6 compares the variability profile in the baseline scenario with those in the last three experiments, characterised by higher precision, lower lifetime and more violence, respectively. By comparing this picture with Figure 2.4, a similar conclusion can be derived as before: the impact of the

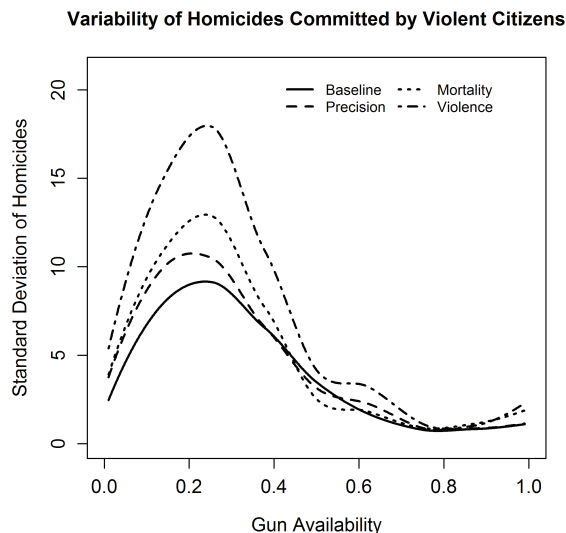


Figure 2.6: Variability of homicides committed for different values of gun availability and different numbers of police officers in the baseline, high precision, low lifetime and high violence scenarios (experiments 1, 3, 4, 5).

considered factors on the standard deviation is analogous to the effect that these variables have on the average number of homicides. In fact, a lower lifetime and a more violent society increase the variability of killings more than the precision of weapons.

Therefore, both Figure 2.5 and 2.6 illustrate a similarity between the behaviour of the level of homicides and the dynamics of their variability.

2.3.5 The Effect of Spatial Concentration

Within the framework of the present model it is also possible to test whether the concentration of people in specific areas, such as a ghetto, increases or decreases the rate of violence and the number of homicides.

In order to perform this test two different scenarios are considered: the case in which citizens are randomly located in the bidimensional space and the one in which they are concentrated in the centre of the lattice (more precisely, in a square whose dimensions are half of those of the lattice). In both situations it is assumed that citizens cannot move.

The model is simulated under these two scenarios assigning to the pa-

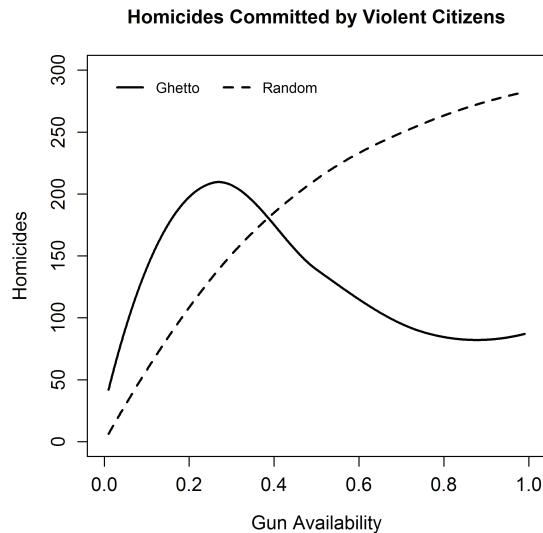


Figure 2.7: Number of homicides committed for different values of gun availability when agents are spatially concentrated and when they are randomly located in the bidimensional space.

rameters the same values of the second experiment, i.e. the one with the larger bidimensional space. The results of the simulations are presented in Figure 2.7.⁵

For low values of the gun availability parameter the number of homicides is higher in the ghetto scenario because in this framework few policemen are inside the space occupied by agents and the number of nonviolent and armed citizens is very low: both these factors strongly favour the activation of potential killers inside the ghetto.

Conversely, for higher values of weapon diffusion, in the spatially concentrated scenario there are many nonviolent citizens endowed with a gun in the centre of the lattice and this lowers the probability of killers' activation: in fact, killers perceive the presence of multiple and potentially armed individuals inside their vision radius. This consideration explains the reason way, in the case of random allocation of agents in the lattice, there are more homicides compared to the alternative scenario when guns are easily available.

⁵The number of policemen employed in these simulations is 50.

2.3.6 More Sophisticated Interactions

The previous agent-based model assumes that there is a complete symmetry between violent and nonviolent citizens in their ability to kill. In fact, violent and nonviolent agents kill and defend themselves, respectively, with the same probability π . In order to prove that this restrictive assumption does not alter the broad conclusions of the model, more realistic forms of interaction are investigated in this subsection.

In particular, it is assumed that armed and violent citizens select their target. Then, what happens next depends on the nature of the victim: if the target is an unarmed citizen, the killer kills him with a probability equal to π_k ; if the victim is armed, with probability π_k the target is killed, but with probability $\pi_v < \pi_k$ the killer can also be suppressed, due to the reaction of the attacked person.

Figure 2.8 shows the total number of killings perpetrated both by killers and by nonviolent citizens for self-defense when $\pi_k = 0.6$ and $\pi_v = 0.1$ (solid line). The hump-shaped profile appears to be preserved even in this scenario, possibly hinting at the fact that the main results of the previous analysis are robust. Interestingly, if the probability π_v assumes a larger value ($\pi_v = 0.6$, dashed line in Figure 2.8) and the self-defence capacity is consequently increased, the total number of killings decreases with respect to the previous scenario in correspondence to medium and low values of gun diffusion, but it increases when α exceeds a certain threshold: this raise of mortality can be ascribed to the gun diffusion that magnifies the likelihood that crimes end up in a bloodshed.

2.4 Concluding Remarks

The present chapter examines the effects of gun availability on firearm-related homicides in an agent-based framework. This simple model can be

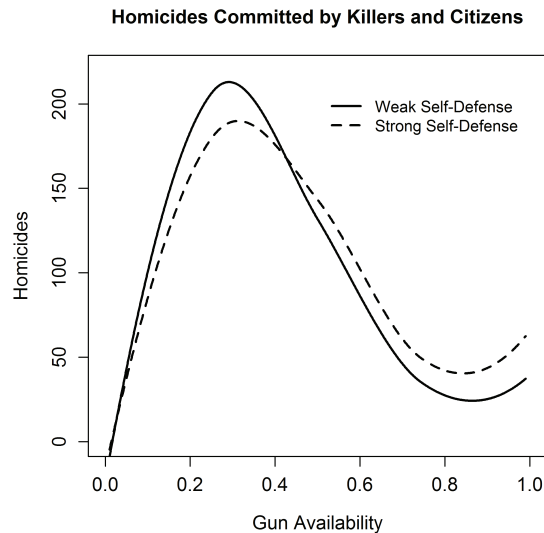


Figure 2.8: Total number of killings perpetrated by killers and by nonviolent citizens for self-defense with more realistic interactions and different self-defense abilities.

used to derive some important policy implications. For instance, when the number of police officers suffices to control the territory, either a complete ban of private weapons or a widespread gun ownership allow to minimise the number of homicides committed. Conversely, when the number of police officers is relatively low, the number of violent deaths is an increasing function of the gun availability parameter and, therefore, the minimum is reached with a diffusion of weapons closed to zero.

This last result is quite problematic due to the difficulties of implementing a zero-gun policy without a significant number of policemen.⁶ Under these circumstances, cultural factors, like a less exacerbated individualism and the preeminence of public forms of defense, may play a fundamental role in reducing the diffusion of guns.

Moreover, the model highlights the trade-off between private and public defense: in fact, a reduction in the number of police officers causes a shift towards private forms of self-defense, especially for relatively high values of gun diffusion. In addition, the model predicts that the number of firearm-related homicides increases more in scenarios characterised by a higher nat-

⁶We thank Ugo Fratesi for pointing this out.

ural mortality, associated also with high birth rates, or in more violent societies rather than in scenarios with more precise and lethal weapons.

Finally, the analysis of simulated data reveals that the variability of homicides clearly tracks their level: this means that the same value of gun availability maximises both the number and the standard deviation of killings, and a violent society is characterised by a higher and more volatile homicide rate than the baseline scenario.

Agent-based modeling is a natural framework to study phenomena in which interactions between many heterogeneous agents play a fundamental role. The problem addressed in this paper clearly falls in this category and this explains the reason why some important results, such as the hump-shaped profile of homicides with respect to gun availability, emerges naturally from the interplay of the different agents, while in the standard analytical models such results usually require artificial and clearly *ad hoc* assumptions.

The proposed methodology also allows to introduce in a quite easy fashion some important elements, such as the presence of police officers and spatial effects, that are difficult to incorporate in standard approaches. These ingredients add realism to the model and increase the reliability of results for policy purposes.

Chapter 3

Distribution Dynamics of Property Crime Rates in the United States

Abstract

Using crime data for the 48 continental and conterminous US states and the distribution dynamics approach, this paper detects two distinct phases in the evolution of the property crime distribution: a period of strong convergence (1971-1980) is followed by a tendency towards divergence and bimodality (1981-2010). Moreover, the analysis reveals that differences in income per capita and police can explain the emergence of a bimodal shape in the distribution of property crime: in fact, after conditioning on these variables, the bimodality completely disappears. This empirical evidence is consistent with the predictions of a two-region model, that stresses the importance of income inequality in determining the dynamics of the property crime distribution.

3.1 Introduction

A huge literature has tried to understand the causes and the dynamics of crime and important contributions can be found in different social science disciplines: from economics (Becker, 1968) to sociology (Cohen and Felson, 1979), from politics (Smith, 1997) to law (Marvell and Moody, 2001). A huge set of determinants has been considered to explain crime, including unemployment, income inequality, police officers, the legalization of abortion, and many others: see, *inter alia*, Cornwell and Trumbull (1994), Marvell and Moody (1996), Kapuscinski *et al.* (1998), Donohue and Levitt (2001), Greenberg (2001), Paternoster and Bushway (2001), Raphael and Winter-Ebmer (2001), Gould *et al.* (2002), Levitt (2002), Machin and Meghir (2004), Baltagi (2006), Rosenfeld and Fornago (2007).

Moreover, the US empirical crime literature has focused its attention on the dynamics of the aggregate level of crime in the United States, such as Cook and Cook (2011). In particular, many papers have tried to explain the raise of crime rates in the 1970s and 1980s and their decline in the 1990s. Reviewing the evidence from these numerous papers, Levitt (2004) identifies four factors that explain the decrease of crime started in the 1990s: the increasing number of policemen, the skyrocketing number of prisoners, the ebbing of the crack epidemic and the legalization of abortion in the 1970s. Another paper trying to explain the dynamics of crime is represented by Shoemith (2010), who uses an error correction model and four factors to explain both the raise and fall of crime rates. The employed factors are arrest rates, income per capita, the proportion of justice resources devoted to drug crime, and alcohol consumption.

The aim of this paper is different because it does not focus on the aggregate value of crime but on the analysis of the entire distribution of property crime rates for the US states and on its evolution over time. Other papers have tried to address this issue using standard approaches, like the beta-

convergence and sigma-convergence concepts: for instance, Cook and Winfield (2013), employing growth regressions and measures of cross-sectional variation, provide evidence of convergence for the US states, whereas, using a different probabilistic approach, Cook and Watson (2013) find different results depending on the period analysed and on the crime typology considered.

However, it has been recognised that a negative relationship between initial values and growth rates, which is the essence of the beta-convergence analysis (Baumol, 1986; Barro, 1991; Barro and Sala-i-Martin, 1991, 1992), is a necessary but not a sufficient condition for convergence (Quah, 1993a): in fact, the regression approach, being inspired by the neoclassical model of growth and focusing on the behaviour of a representative economy towards its own steady state, is completely silent on what happens to the entire cross-sectional distribution. Moreover, the sigma-convergence analysis (Sala-i-Martin, 1996) is also affected by significant drawbacks because, as argued by Quah (1996a), a constant variability is compatible with very different dynamics, from criss-crossing and leap-frogging to persistent inequality. Distinguishing between these completely different patterns is crucial and is possible only by analysing the entire cross-sectional distribution.

In order to overcome these criticisms affecting the existing literature about convergence analysis of crime, the present paper adopts an alternative methodology, i.e. the distribution dynamics approach (Quah, 1993a and b, 1996a and b, 1997), which allows the study of the entire distribution of crime rates, both in terms of shape and of intra-distributional dynamics.

In particular, this paper considers the dynamics of property crime rates for 48 conterminous US states during the period 1971-2010. Results indicate different phases for this typology of crime: in fact, a period of strong convergence (1971-1980) is followed by a tendency towards divergence and bimodality (1981-2010).

Furthermore, the analysis reveals that differences in the levels of income

per capita, whose divergence starting from the 1980s has been documented by Gerolimetto and Magrini (2014) in a distribution dynamics setting, and in the numbers of state police employees, which also exhibit a divergent pattern starting from the 1980s, can explain the emergence of a bimodal shape in the distribution of property crime rates: in fact, after conditioning on these two variables, the bimodality completely disappears.

The rest of the chapter is organised as follows: Section 3.2 presents a two-region model which investigates the relationships between crime and other socio-economic variables from a theoretical point of view; Section 3.3 introduces the adopted empirical methodology, whereas Section 3.4 describes the data employed; Sections 3.5-3.7 present the empirical results obtained with the distribution dynamics technique and explore the relationship between crime and some of its determinants; finally, Section 3.8 concludes.

3.2 A Two-Region Model of Crime Dynamics

This section presents a theoretical framework in which it is possible to explore the dynamics of crime over time and across different spatial units.

In particular, in this model there are two regions or states, indicated by A and B . In each state $i \in \{A, B\}$ and at each time $t \in \{1, 2, \dots, T\}$, the number of property crimes committed is denoted by $c_{i,t}$. The evolution of property crime in each region depends on its past value $c_{i,t-1}$, on the number of police resources $p_{i,t}$ and on the level of after-tax income $(1 - \tau_{i,t}) y_{i,t}$:

$$c_{i,t} = (1 + \rho) c_{i,t-1} - \psi p_{i,t} - \sigma (1 - \tau_{i,t}) y_{i,t} \quad (3.1)$$

where ρ is the growth rate of crime when police and income are both zero, while ψ and σ measure how much crime is sensible to current variations of police resources and after-tax income, respectively. The reason for this

specification is very intuitive: a higher level of police resources means more crime repression activities, whereas a higher value of legal income makes crime less attractive. Moreover, this specification is consistent with economic models of crime, such as Becker (1968), which show that individuals tend to commit crime when the probability of punishment or the opportunities in the legal labour market are low.

On the other hand, the future value of income depends on the current level of crime, because the presence of high crime rates reduces the resources available in each state by discouraging investments:

$$y_{i,t+1} = (1 + \theta) y_{i,t} - \omega c_{i,t} + \eta_{i,t+1} \quad (3.2)$$

in which θ is the growth rate of income in the absence of crime, ω measures how much income is sensible to current variations of crime, and, finally, $\eta_{i,t+1}$ is an exogenous, independently distributed shock with zero-mean, capturing all the future positive or negative surprises (e.g. unexpected increase or decrease of labour productivity).

The two states decide, through taxation, the share of resources $\tau_{i,t}$ to allocate to police:

$$p_{i,t} = \tau_{i,t} y_{i,t} \quad (3.3)$$

Consequently, the expenditure in crime repression improves the future level of income by reducing crime and its negative effect on the level of resources, but it is a costly investment because it requires an increase of the tax rate.

It is assumed that politicians choose in each period the level of taxation by maximising the probability of being re-elected Π , which is a strictly increasing function of the expected economic performance minus the current

costs of taxation:¹

$$\max_{\tau_{i,t}} \Pi \left(\delta E_{i,t}(y_{i,t+1}) - \phi \frac{\tau_{i,t}^2}{2} \right) \quad (3.4)$$

where $\Pi'(\cdot) > 0$, $E_{i,t}(\cdot)$ is the expected value conditioned on the information set available at time t in state i , while δ and ϕ are the two weights associated to the expected future economic performance $E_{i,t}(y_{i,t+1})$ and the political costs of taxation $\frac{\tau_{i,t}^2}{2}$, respectively.

The first order conditions of the problem can be rewritten in the following way:

$$\phi \tau_{i,t} = \omega \delta (\psi - \sigma) y_{i,t} \quad (3.5)$$

in which the left-hand side represents the marginal cost of taxation, whereas the right-hand side is the marginal benefit. It is worth noting that taxation has a positive benefit only if the crime sensitivity to police, measured by ψ , is higher than the degree of dependence on after-tax income, indicated by σ .

The optimal level of taxation equalizes marginal benefits and marginal costs:

$$\tau_{i,t}^* = \frac{\omega \delta (\psi - \sigma) y_{i,t}}{\phi} \quad (3.6)$$

This expression shows that the optimal tax is higher when: the weight associated to taxation, measured by ϕ , is lower; the net benefit of taxation $(\psi - \sigma) y_{i,t}$ is higher; income is more sensitive to crime, as indicated by ω ; the effect of the economic performance on the probability of being re-elected δ is higher. Substituting the last quantity in the equation of crime, income and police, it is possible to obtain the optimal dynamics for these three variables. In the model calibration, it is reasonably assumed that the net benefit of taxation is positive ($\psi = 0.08, \sigma = 0.05$) and that the probability of being re-elected is more sensible to the economic performance than the

¹For simplicity, it is assumed that elections take place at the end of each period. In fact, this assumption allows to derive solutions in closed form simplifying the analysis of the model.

cost of taxation ($\delta = 0.95, \phi = 0.35$).

This model allows to analyse the effects of an exogenous income shock and its propagation to the other variables of the system. In particular, the case of an increase in income inequality is considered because this scenario is related to the increasing inequality in terms of income per capita observed across the US states, starting from the 1980s. Consequently, it is assumed in the main calibration that state A is the richest region ($y_{A,0} = 18 > y_{B,0} = 16$), which also starts with the highest level of crime ($c_{A,0} = 13 > c_{B,0} = 11$). The growth rates of income and crime are $\theta = 0.05$ and $\rho = 0.085$, respectively, and the sensitivity of income to crime is $\omega = 0.06$. The two regions are followed for 40 periods ($T = 40$) to mimic the forty years considered in the next empirical analysis, i.e. the period from 1971 to 2010.² It is assumed that the richest region has the highest number of crimes committed because this is consistent with the data, showing a positive correlation between property crime and income per capita at the beginning of the 1970s. Moreover, the shocks $\eta_{i,t}$ are always zero, except for region A at time 10, and the analysis considers a low (1.8), medium (2.6) and high value (3.8) of the shock $\eta_{A,10}$. Table 3.1 summarises the values chosen for the model parameters.

Figure 3.1 reports the dynamics implied by the model for the main variables in the different scenarios considered. In particular, the columns correspond to the small, medium and big shock scenario, respectively. The first row shows the timing and magnitude of the shock; the second and third rows present the dynamics over time of income and crime in the two regions, compared to the average of the two states in each period, respectively (the time series of tax rate and police have the same pattern of income and, for

²The model and its predictions have been conceived to be valid for a finite time horizon, such as 40 years, in order to be tested in the next empirical analysis with US crime data from 1971 to 2010. It is worth stressing that long-run steady state implications cannot be derived from the proposed approach. In fact, the model is unbounded in the long term, but still it is suggestive to explore a transient phase lasting for about half a century. We thank Matteo Richiardi for pointing this out.

Parameter	Interpretation	Value
T	Time horizon	40
ρ	Crime growth rate	0.085
ψ	Crime sensitivity to police	0.08
σ	Crime sensitivity to income	0.05
θ	Income growth rate	0.05
ω	Income sensitivity to crime	0.06
δ	Re-election sensitivity to income	0.95
ϕ	Re-election sensitivity to taxation	0.35
$c_{A,0}$	Initial crime in region A	13
$c_{B,0}$	Initial crime in region B	11
$y_{A,0}$	Initial income in region A	18
$y_{B,0}$	Initial income in region B	16
$\eta_{A,10}$	Income shock in region A at time 10	$\{1.8, 2.6, 3.8\}$

Table 3.1: Values chosen for the parameters of the model.

this reason, are omitted); finally, the last row depicts the trajectory of the aggregate value of crime, which is the sum of the crime levels in the two regions. In every scenario the mechanism behind the model is the same: a higher (lower) level of income leads to a decline (raise) of crime through both the opportunity cost and the police channel.

In the case of a small shock affecting the income of the richest region, this state has not enough resources to reduce its crime level, which continues to grow and subtract wealth to the state, and this leads to a divergent crime pattern. Moreover, the aggregate level of crime exhibits an explosive trend due to the strong growth of crime in both regions.

On the other hand, the second column shows that a bigger income shock provides to state A enough resources to limit the growth of its crime level: as a consequence, the time series of crime in the two regions converge to their average at the end of the forty periods considered. However, the aggregate level of crime presents an increasing linear trend.

Finally, with an even bigger shock, the dynamics of the system changes completely: in this scenario the richest region is able to reduce its crime level compared to the poorest region. Benefiting from this crime reduction, income in region A displays an increasing pattern, which also leads to a

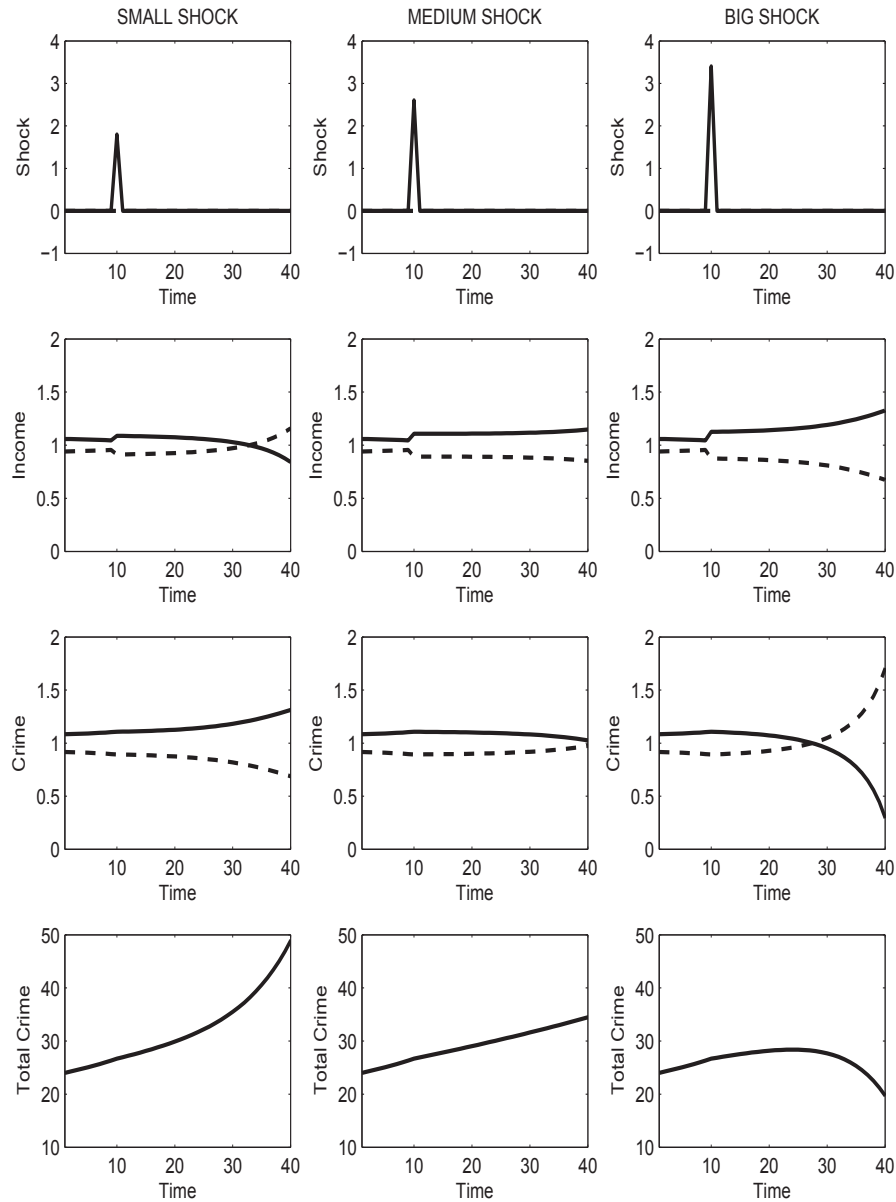


Figure 3.1: Time series of the main variables of the model in the presence of different income shocks in region A (solid line) and in region B (dashed line): income shock (first panel); relative income in the two regions (second panel); relative crime in the two regions (third panel); sum of the crime levels in the two regions (fourth panel).

greater inequality in the available resources. Since the richest region is able to lower its crime level more than the poorest state, the result is that the two crime trajectories converge in a first phase, but then they diverge in the final periods. Furthermore, looking at the aggregate value of crime in the two states, an increasing trend in the first periods is followed by a decline, because the decrease of crime in region A is larger than the increase in state B .

If the values assigned to the weight of taxation ϕ , the income sensitivity to crime ω , or the crime growth rate ρ are increased, results gradually change towards a divergence of the distribution of crime in the two states and to an explosive trend in the aggregate level of crime. The same happens if the crime sensitivity to police ψ and after-tax income σ , the effect of economic performance on the probability of re-election δ , or the income growth rate θ are reduced.

The three scenarios considered reveal that, from a theoretical point of view, a greater income inequality between regions, such as the one experienced in the US starting from the 1980s, can have completely different consequences on the dynamics of crime and on its distribution, depending on the size of the shocks that drive this phenomenon. The following empirical analysis will reveal which theoretical scenario best approximates the US experience.

3.3 Methodology

The aim of this section is to provide a brief technical description of the methodology chosen to analyze convergence, i.e. the distribution dynamics approach, and the reasons why this methodology is preferred to standard methods, like the beta- and sigma-convergence concepts.

3.3.1 Distribution Dynamics Approach

As mentioned in the Introduction of this chapter, there are two approaches to the analysis of convergence: the regression approach (beta-convergence), complemented by the study of the cross-sectional variability (sigma-convergence), and the distribution dynamics method. In this paper the latter approach is chosen because it allows the study of the entire cross-sectional distribution of a given variable, both in terms of external shape and intra-distributional dynamics, using stochastic kernels to describe its evolution over time. This paragraph provides a brief description of the adopted methodology.

Let c_t and c_{t+s} represent the crime rates, relative to the group average, of a set of n states at time t and $t+s$, respectively. Moreover, assuming that the two random variables admit a density, denoted by $f(c_t)$ and $f(c_{t+s})$, and that $f(\cdot)$ can be modeled as a first order process, the density at time $t+s$ is given by:

$$f(c_{t+s}) = \int_{-\infty}^{+\infty} f(c_{t+s}|c_t)f(c_t)dc_t \quad (3.7)$$

in which $f(c_{t+s}|c_t)$ is the conditional density function that maps the values at time t into the values at time $t+s$. This density function is called stochastic kernel and it plays a crucial role within this approach: in fact, it provides information on the movements from one part of the distribution to another one between time t and $t+s$. For this reason, once the stochastic kernel is estimated, convergence can be analysed directly from its shape or, assuming a time homogeneous markov process for the studied phenomenon, by comparing the initial distribution at time t to the so-called ergodic distribution, which is the limit of $f(c_{t+s})$ when s goes to infinity. In more intuitive terms, the ergodic distribution is the characterisation of the likely long-run cross-sectional distribution of the variable of interest.

Observing a given variable c on a set of n statistical units at two points in time, t and $t+s$, the easiest way to estimate the stochastic kernel is

through the kernel density estimator, which takes the following expression:

$$\hat{f}(c_{t+s}|c_t) = \frac{\hat{f}(c_{t+s}, c_t)}{\hat{f}(c_t)} \quad (3.8)$$

where the kernel estimator of the the joint density function is:

$$\hat{f}(c_{t+s}, c_t) = \sum_{i=1}^n \frac{1}{nh_{c_{t+s}}h_{c_t}} K\left(\frac{c_{t+s} - c_{i,t+s}}{h_{c_{t+s}}}\right) K\left(\frac{c_t - c_{i,t}}{h_{c_t}}\right) \quad (3.9)$$

and the kernel density estimator of the initial density is:

$$\hat{f}(c_t) = \sum_{i=1}^n \frac{1}{nh_{c_t}} K\left(\frac{c_t - c_{i,t}}{h_{c_t}}\right) \quad (3.10)$$

in which $K(\cdot)$ is a kernel function and h is a chosen bandwidth parameter that controls the degree of smoothing applied to the density estimate.

However, as argued by Hyndman *et al.* (1996), this estimator might have poor properties in terms of bias: the authors propose to adjust the estimate of the mean function implicit in the kernel density estimator with one obtained from a smoother with better bias properties. For this reason, according to Loader (1999), the local linear estimator should be chosen in the analysis. Following Gerolimetto and Magrini (2014), in order to estimate the conditional density, a Gaussian kernel is selected with a nearest-neighbour bandwidth in the initial year dimension, with a span of 30% of the data, and a fixed Normal Scale bandwidth, as suggested by Silverman (1986), in the final year dimension. The local linear estimator for the mean function has a nearest-neighbour bandwidth with a span chosen to minimise the AIC criterion.

The output of this type of analysis is represented by a set of figures: (i) a three-dimensional plot of the estimated stochastic kernel; (ii) the corresponding contour plot, highlighting the contours at the 90%, 50% and 10% level; (iii) the Highest Density Regions (HDR) plot, proposed by Hyndman

(1996), in which the vertical strips represent conditional densities given specific values for the initial year and, for each strip, darker to lighter areas indicate the 10%, 50% and 90% highest density regions; (iv) a graph comparing the initial year distribution with the final year one and the ergodic.

Then, convergence is analysed by looking at the three-dimensional shape of the stochastic kernel and at the corresponding contour and HDR plots or by comparing the initial distribution with the final one and the ergodic. In more detail, a probability mass located along the main diagonal in the contour and HDR plots indicates a persistence feature of the studied phenomenon, because the elements in the cross-sectional distribution remain where they started. On the other hand, a convergence process is highlighted by a probability mass concentrated around the mean value at time $t + s$ and parallel to the time t axis, while a distribution parallel to the $t + s$ axis is a signal of divergence: in fact, in the first case, the units of analysis, characterised by different values at time t , will exhibit a similar value at time $t + s$, whereas, in the second case, the opposite behaviour is observed. Finally, the formation of two, or more, modes in the ergodic distribution reveals a tendency towards polarization or stratification.

3.3.2 Criticisms of Other Approaches

This subsection provides a brief motivation of the reasons why the distribution dynamics approach should be preferred to standard methodologies, like the beta-convergence (Baumol, 1986; Barro, 1991; Barro and Sala-i-Martin, 1991, 1992) and sigma-convergence analysis (Sala-i-Martin, 1996).

Essentially, the beta-convergence aims at testing the convergence of a given process by looking at a negative correlation between the initial values of the studied variable and its growth rates: if statistical units with high values in the initial period show lower growth rates than units with low values, this should mean that they converge to a common steady state.

However, it has been recognised that a negative relationship between initial values and growth rates is a necessary but not a sufficient condition for convergence (Quah, 1993a): this is because the regression approach, by focusing on the behaviour of a representative unit towards its own steady state, is completely silent on what happens to the entire cross-sectional distribution of the studied statistical units.

Thus, it has been suggested to complement the beta-convergence approach with the study of the cross-sectional variability over time (sigma-convergence): the idea is that a reduction of the standard deviation of the distribution, together with a negative relationship between initial values and growth rates, should be a sufficient signal of convergence among the units of interest. Indeed, as argued by Quah (1996a), a constant variability is compatible with very different behaviours, from criss-crossing and leap-frogging to persistent inequality. Distinguishing between these completely different dynamics is crucial and it is possible only by analysing the entire cross-sectional distribution.

3.4 Data

The crime data used in this paper are from the Federal Bureau of Investigation (FBI)'s Uniform Crime Reports (UCR),³ which include crime reports submitted voluntarily either directly by local, state, federal or tribal law enforcement agencies or through centralised state agencies across the country. Data are freely available online for each year, starting from 1960, and for the 50 US states, plus the District of Columbia. Crimes are classified according to the following categories: burglary, larceny-theft, motor-vehicle theft, murder, rape, robbery, assault. The first three typologies are grouped in the property crime category while the others are classified as violent crimes. The attention of this paper is devoted to the aggregate category of prop-

³Data on property crime rates are available at <http://www.ucrdatatool.gov/>.

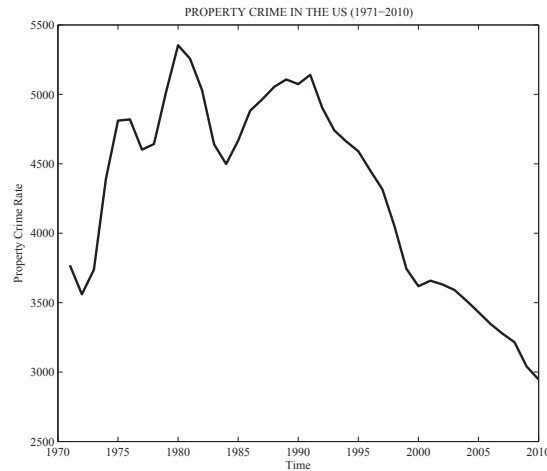


Figure 3.2: Time series of the property crime rate in the US from 1971 to 2010.

erty crime, which is measured by a standard index, the property crime rate, defined as the number of reported property crimes committed per 100,000 inhabitants.

Figure 3.2 plots the time series of the property crime rate in the US. This picture shows a very well-known pattern in the crime literature: the aggregate level of property crime increases up to the beginning of the 1990s and then falls. It is worth stressing that this trend seems consistent with the predictions of the model in the third theoretical scenario of Figure 3.1.

The UCR data have many advantages: they cover a long period of time with a stable methodology, allowing a meaningful trend analysis; they are the only source of geographically disaggregated crime data available for the US; they offer a good coverage in terms of crime typologies and in terms of geographic locations considered. On the other hand, the UCR program has some limitations: it covers only crime reported to the police and many crimes are reported in low percentages; furthermore, since reporting is voluntary, some enforcement agencies may not report information or information may be incomplete. In the presence of incomplete data, the FBI uses specific protocols to impute the missing values: the imputation is based on crime rates of agencies considered similar according to population size,

type of agencies (city, rural and state, suburban counties) and geographic location.⁴

In order to bring the model to the data, a measure of income and police is needed. The relationship between property crime and income will be explored in the following analysis using data on real per capita personal income: the personal per capita income net of current transfer receipts comes from the Bureau of Economic Analysis,⁵ while the consumer price index (CPI) used to deflate income is from the Bureau of Labor Statistics.⁶ On the other hand, the level of crime repression activities in each state is measured by the number of state police employees per 100,000 inhabitants, as recorded in the UCR data.⁷ Furthermore, our analysis is restricted to the forty-year period from 1971 to 2010⁸ and to the 48 continental and conterminous US states.⁹

Figure 3.3 shows the Moran scatterplot map and significance map (Anselin, 1995) of property crime for these states in 1971 and 2010, highlighting with different colours the four types of local spatial association: locations with a high value of crime, with respect to the cross-sectional average, associated to neighbours with high values (HH); states with a high value located

⁴For a more detailed description of the UCR program, in particular, and of crime reports and statistics, in general, see Rennison (2009).

⁵Data on personal per capita income are available at http://www.bea.gov/iTable/index_regional.cfm.

⁶The time series of the CPI index is available at <http://www.bls.gov/cpi/>.

⁷The number of state police employees is reported in the annual publications of the Uniform Crime Reports: to the best of our knowledge, for the earliest periods only the paper version is available (at <https://archive.org/index.php>). There are missing values for some states in few years: in the period from 1968 to 2013, 1.3% of the data are missing. To overcome this problem, in this study, the missing values have been imputed in two ways: by replacing them with the average of the values of the two closest years or, if the missing value is at the end of the period considered, by forecasting it using an ARIMA model. Moreover, in order to have a coherent measure of state police employees, only the police agencies that report their employment since the beginning of the period analysed have been considered.

⁸This choice is motivated by a lack of observations for the New York state in the period 1960-1964 and by the use of out-of-sample lags and leads in the next conditioning procedure.

⁹Therefore, the state of Alaska and the Hawaii are excluded from the sample, as well as the District of Columbia. These states have been excluded to make the results of the present analysis comparable to those of other studies focusing on the continental US states, such as Gerolimetto and Magrini (2014).

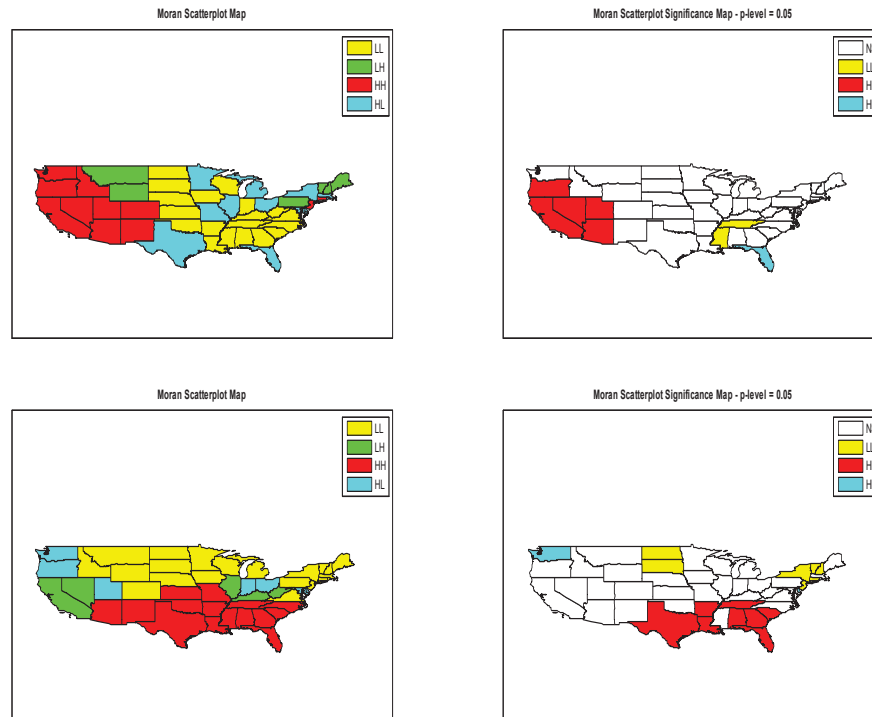


Figure 3.3: Moran scatterplot map (left) and significance map (right) of property crime rates in 1971 (top) and 2010 (bottom).

around neighbours with low values (HL); regions with a low value of crime associated to neighbours with high values (LH); finally, locations with a low value located around neighbours with low values (LL). These maps show that in 1971 property crimes are concentrated in the south-west region with a significant group of states, represented by California and its neighbours, characterised by high crime rates. In 2010 the situation changes: high levels of property crime are visible in the south-east, with a significant cluster that includes Texas, Florida and their neighbours. However, the prevalence of the white colour in the significance map, indicating spatial associations that are not statistically significant, suggests that the data considered are not strongly affected by spatial autocorrelation.

3.5 Distribution Dynamics of Property Crime

Using the methodology described in Section 3.3, the dynamics over time of the distribution of property crime is analysed.

Figure 3.4 shows the results for the overall period, from 1971 to 2010. The first three graphs are related to the shape of the estimated stochastic kernel. In particular, if we look at the contour levels and at the 45 degree line, it is possible to analyse the intra-distributional dynamics between the two considered periods: observations with a high property crime rate in 1971 are likely to have a lower crime rate in 2010; states with a low rate in the initial year tend to present a higher crime rate in the final year; moreover, there is a group of states located around the mean in the initial year experiencing the highest crime rates in the final period. This situation results in a final and ergodic distribution affected by bimodality, as displayed in the fourth graph.¹⁰ The states that are responsible for the first mode of the final density are those located in the northern part of the US while the second mode can be attributed to the states in the south-east.

However, behind this dynamics, two distinct phases are identifiable.¹¹ In fact, Figure 3.5 depicts a period of strong convergence from 1971 to 1980, made evident by a sharply concentrated unimodal ergodic distribution and by a noticeable clockwise rotation of the estimated probability mass: this rotation represents evidence of convergence because it implies that states with a low crime rate at the beginning of the period considered present higher rates at the end; and the opposite holds for states with high crime rates. Conversely, Figure 3.6 shows a phase of divergence, from 1981 to 2010, in which the distribution of property crime rates shows a clear ten-

¹⁰The bimodal shape is confirmed by the formal Silverman's (1981) test performed on the final distribution, whose shape is very close to that of the ergodic distribution.

¹¹The split between the two periods, 1971-1980 and 1981-2010, is obtained as a result of a statistical analysis aimed at detecting a structural break. In particular, the forty-year period from 1981 to 2010 has been divided in four decades and the distribution dynamics analysis has been applied to each of them. Then, the decades with a similar convergent or divergent behaviour have been aggregated.

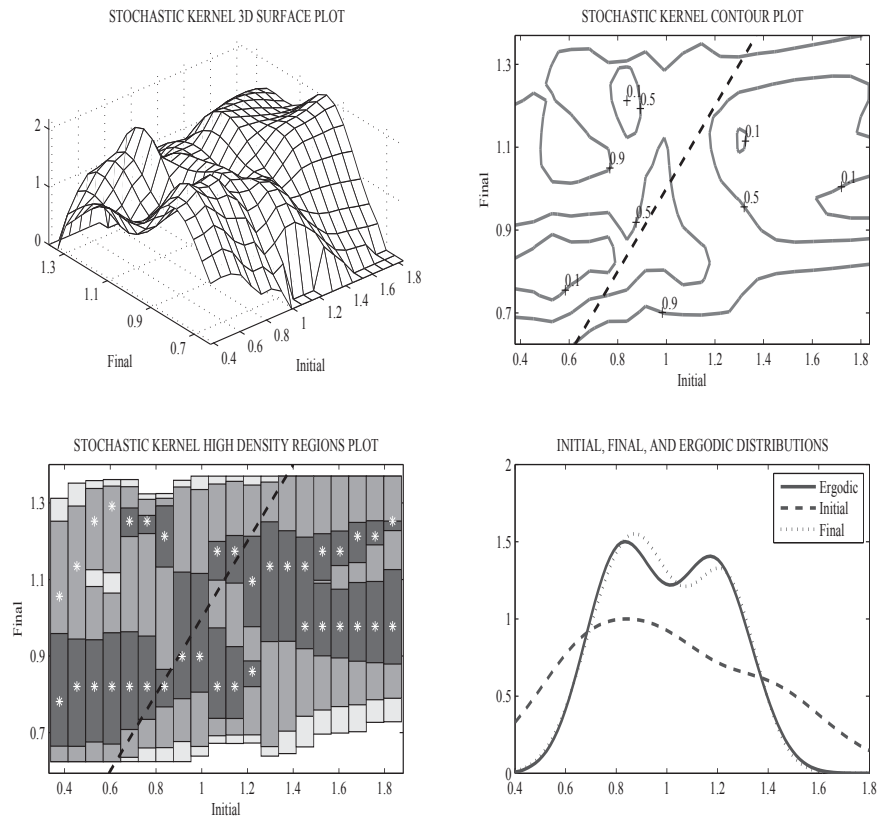


Figure 3.4: Distribution dynamics analysis of property crime rates for the period 1971-2010 using the 48 continental US states. A three-dimensional plot of the estimated stochastic kernel (top-left); the corresponding contour plot, highlighting the contours at the 90%, 50% and 10% level (top-right); the Highest Density Regions (HDR) plot (bottom-left); a graph comparing the initial year and the final year distribution with the ergodic distribution (bottom-right). *Notes:* estimates of the stochastic kernel adopt a nearest-neighbour bandwidth in the initial year dimension with a span equal to 0.3, a Normal Scale (Silverman, 1986) bandwidth in the final year dimension and a Gaussian kernel. The mean bias adjustment (Hyndman *et al.*, 1996) is obtained using a local linear estimate with a nearest-neighbour bandwidth, whose span is chosen in order to minimise the AIC. In contour and HDR plots, the dashed line indicates the main diagonal, the asterisks represent the modes.

gency towards bimodality, made transparent by the comparison of the initial distribution with the final one and the ergodic.

3.6 Robustness Checks

These findings seem to suggest a dynamics more similar to the third scenario predicted by the model. In order to test the robustness of the obtained results and to address the concern that a particular city or county is driving the whole of the distribution (e.g. the city of New York in the state of New York), the analysis is replicated considering the 9 regions in which the US territory is divided according to the definition of the United States Census Bureau.

Figure 3.7 presents the distribution dynamics analysis for these regions in the period 1971-1980: convergence is highlighted by a clockwise rotation of the probability mass and by the transition from an initial distribution characterised by high variability to a more concentrated, although bimodal, final distribution. A further evidence of convergence is represented by the ergodic distribution which exhibits lower variability than the final distribution and in which any evidence of bimodality disappears. Figure 3.8 replicates this exercise for the period 1981-2010: the last picture in this figure reveals the emergence of a final and ergodic distribution far less concentrated than the initial one. With only 9 regions it is not possible to capture the bimodal shape observed in Figure 3.6; however, the tendency towards divergence is clear.

The analysis performed on more aggregated regional divisions proves the robustness of the results regarding the existence of two phases in the evolution of the distribution of property crime, i.e. a period of convergence followed by a divergent dynamics.¹² This evidence is again consistent with

¹²Moreover, it is possible to affirm that the main results are robust to changes in the scale used in the analysis (states or regions).

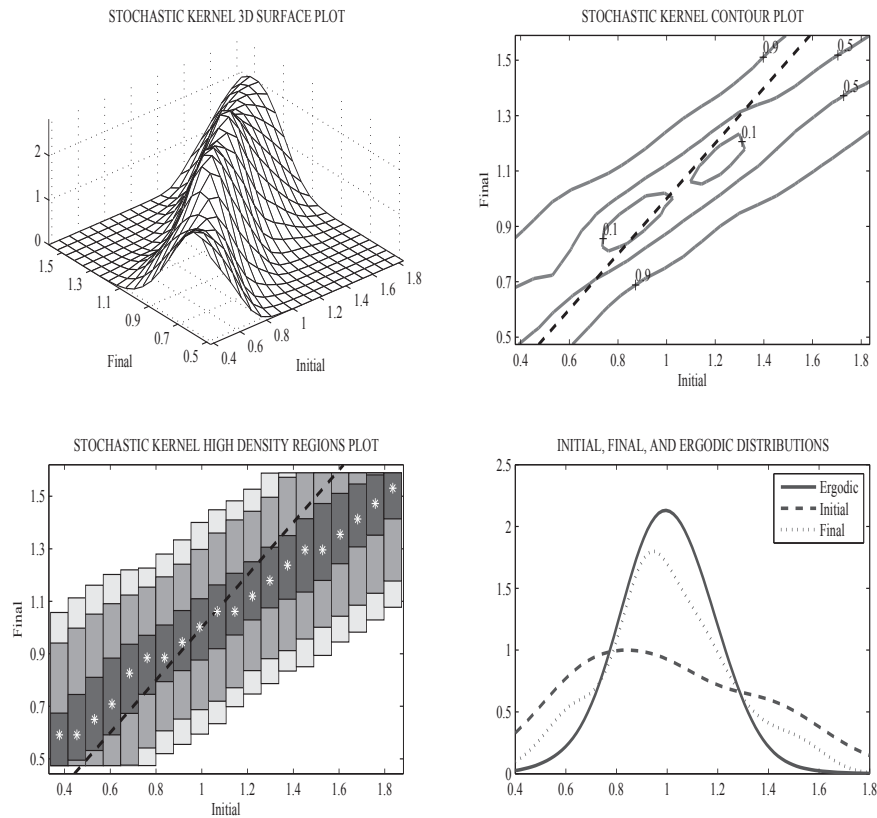


Figure 3.5: Distribution dynamics analysis of property crime rates for the period 1971-1980 using the 48 continental US states. A three-dimensional plot of the estimated stochastic kernel (top-left); the corresponding contour plot, highlighting the contours at the 90%, 50% and 10% level (top-right); the Highest Density Regions (HDR) plot (bottom-left); a graph comparing the initial year and the final year distribution with the ergodic distribution (bottom-right). *Notes:* estimates of the stochastic kernel adopt a nearest-neighbour bandwidth in the initial year dimension with a span equal to 0.3, a Normal Scale (Silverman, 1986) bandwidth in the final year dimension and a Gaussian kernel. The mean bias adjustment (Hyndman *et al.*, 1996) is obtained using a local linear estimate with a nearest-neighbour bandwidth, whose span is chosen in order to minimise the AIC. In contour and HDR plots, the dashed line indicates the main diagonal, the asterisks represent the modes.

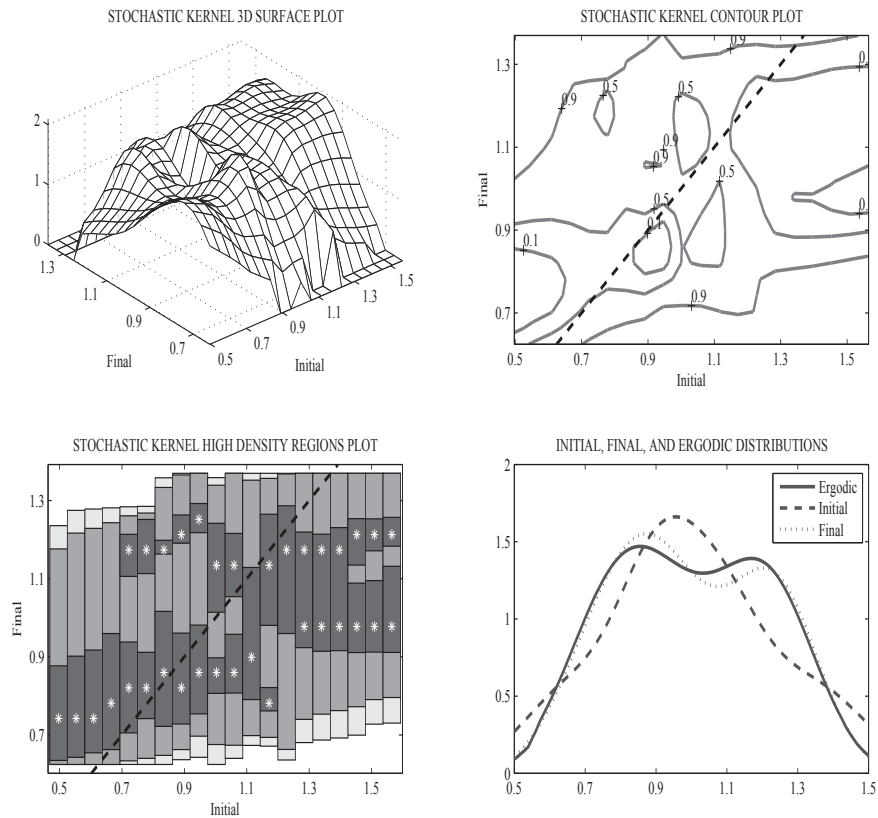


Figure 3.6: Distribution dynamics analysis of property crime rates for the period 1981-2010 using the 48 continental US states. A three-dimensional plot of the estimated stochastic kernel (top-left); the corresponding contour plot, highlighting the contours at the 90%, 50% and 10% level (top-right); the Highest Density Regions (HDR) plot (bottom-left); a graph comparing the initial year and the final year distribution with the ergodic distribution (bottom-right). *Notes:* estimates of the stochastic kernel adopt a nearest-neighbour bandwidth in the initial year dimension with a span equal to 0.3, a Normal Scale (Silverman, 1986) bandwidth in the final year dimension and a Gaussian kernel. The mean bias adjustment (Hyndman *et al.*, 1996) is obtained using a local linear estimate with a nearest-neighbour bandwidth, whose span is chosen in order to minimise the AIC. In contour and HDR plots, the dashed line indicates the main diagonal, the asterisks represent the modes.

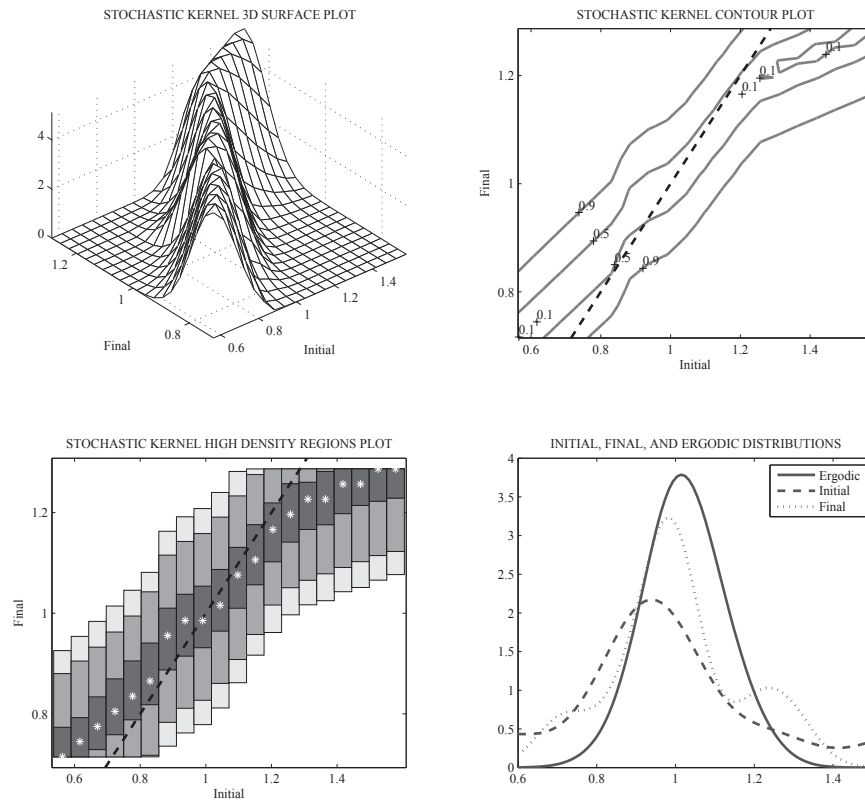


Figure 3.7: Distribution dynamics analysis of property crime rates for the period 1971-1980 using the 9 US regions. A three-dimensional plot of the estimated stochastic kernel (top-left); the corresponding contour plot, highlighting the contours at the 90%, 50% and 10% level (top-right); the Highest Density Regions (HDR) plot (bottom-left); a graph comparing the initial year and the final year distribution with the ergodic distribution (bottom-right). *Notes:* estimates of the stochastic kernel adopt a bandwidth selected with the direct plug-in method in the initial year dimension, a Normal Scale (Silverman, 1986) bandwidth in the final year dimension and a Gaussian kernel. The mean bias adjustment (Hyndman *et al.*, 1996) is obtained using a local linear estimate with a nearest-neighbour bandwidth, whose span is chosen in order to minimise the AIC. In contour and HDR plots, the dashed line indicates the main diagonal, the asterisks represent the modes.

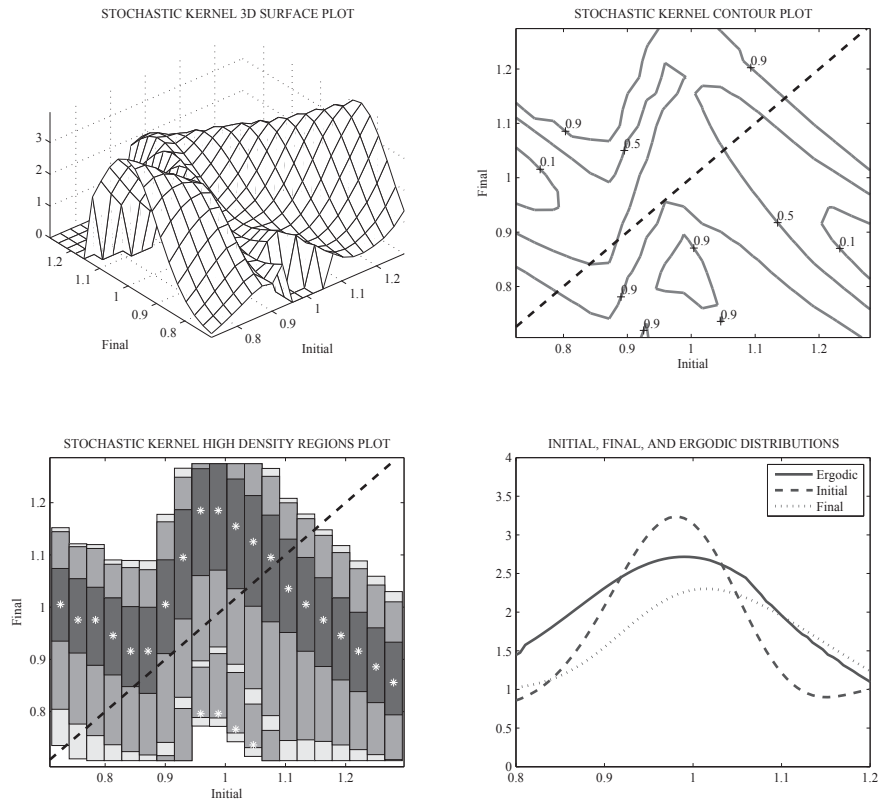


Figure 3.8: Distribution dynamics analysis of property crime rates for the period 1981-2010 using the 9 US regions. A three-dimensional plot of the estimated stochastic kernel (top-left); the corresponding contour plot, highlighting the contours at the 90%, 50% and 10% level (top-right); the Highest Density Regions (HDR) plot (bottom-left); a graph comparing the initial year and the final year distribution with the ergodic distribution (bottom-right). *Notes:* estimates of the stochastic kernel adopt a bandwidth selected with the direct plug-in method in the initial year dimension, a Normal Scale (Silverman, 1986) bandwidth in the final year dimension and a Gaussian kernel. The mean bias adjustment (Hyndman *et al.*, 1996) is obtained using a local linear estimate with a nearest-neighbour bandwidth, whose span is chosen in order to minimise the AIC. In contour and HDR plots, the dashed line indicates the main diagonal, the asterisks represent the modes.

the third scenario predicted by the model, characterised by the presence of strong income shocks.

3.7 Conditional Distribution Dynamics

According to the theoretical framework of Section 3.2, the divergence of property crime rates is driven by income shocks that affect crime through the channels of opportunity cost and police. Moreover, in the same period in which a tendency towards bimodality has been detected for property crime rates, i.e. the years from 1981 to 2010, Gerolimetto and Magrini (2014) find an analogous divergent pattern using real per capita personal income for the same 48 conterminous US states: in fact, the ergodic distribution of income in the last picture of Figure 3.9 presents a higher concentration in the right tail than the initial one. By applying the distribution dynamics technique, the same divergent tendency can be observed in the number of state police employees, starting from the 1980s: Figure 3.10 shows this feature. These considerations motivate the idea to explore more deeply the relationship between income, police and crime from an empirical point of view.

In order to understand if income and police can explain the bimodality of property crime, the conditional distribution of the variable of interest must be considered. Since both income and police are likely to be endogenous variables,¹³ the method proposed by Quah (1996b) is considered in the following analysis.

The first step of the procedure consists in estimating a growth regression, in which the growth rate of the dependent variable is regressed on a set of potentially endogenous variables, and then taking the fitted values for subsequent analysis: in order to consider the possible endogenous nature of these variables and, in particular, the presence of feedback effects, both the

¹³In states with high crime rates there might be less investments and, hence, lower income. Moreover, the higher the crime rate is, the more a state should be willing to invest in police and crime repression.

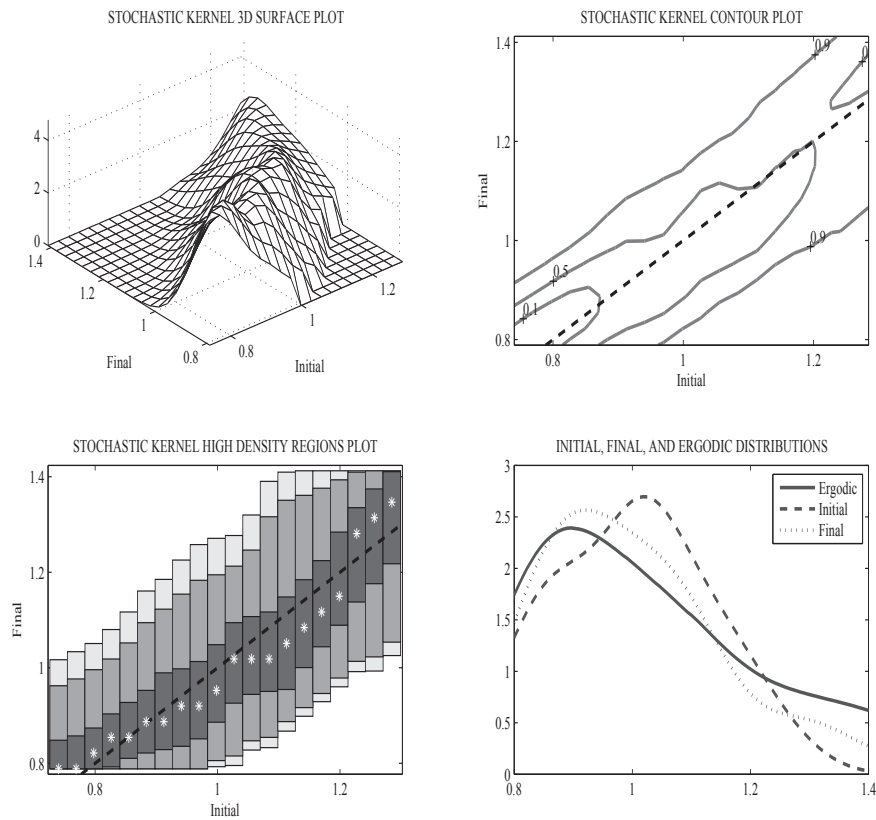


Figure 3.9: Distribution dynamics analysis of real per capita personal income for the period 1981-2010 using the 48 continental US states. A three-dimensional plot of the estimated stochastic kernel (top-left); the corresponding contour plot, highlighting the contours at the 90%, 50% and 10% level (top-right); the Highest Density Regions (HDR) plot (bottom-left); a graph comparing the initial year and the final year distribution with the ergodic distribution (bottom-right). *Notes:* estimates of the stochastic kernel adopt a nearest-neighbour bandwidth in the initial year dimension with a span equal to 0.3, a Normal Scale (Silverman, 1986) bandwidth in the final year dimension and a Gaussian kernel. The mean bias adjustment (Hyndman *et al.*, 1996) is obtained using a local linear estimate with a nearest-neighbour bandwidth, whose span is chosen in order to minimise the AIC. In contour and HDR plots, the dashed line indicates the main diagonal, the asterisks represent the modes.

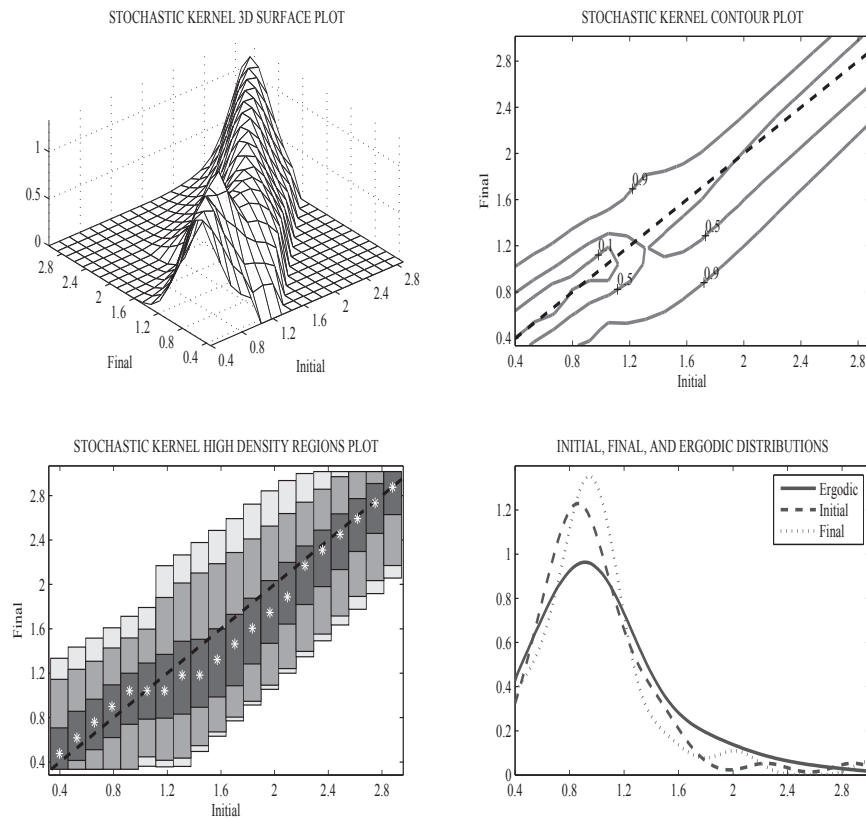


Figure 3.10: Distribution dynamics analysis of state police employees per 100,000 inhabitants for the period 1981-2010 using the 48 continental US states. A three-dimensional plot of the estimated stochastic kernel (top-left); the corresponding contour plot, highlighting the contours at the 90%, 50% and 10% level (top-right); the Highest Density Regions (HDR) plot (bottom-left); a graph comparing the initial year distribution with the final year one and the ergodic (bottom-right). *Notes:* estimates of the stochastic kernel adopt a nearest-neighbour bandwidth in the initial year dimension with a span equal to 0.3, a Normal Scale (Silverman, 1986) bandwidth in the final year dimension and a Gaussian kernel. The mean bias adjustment (Hyndman *et al.*, 1996) is obtained using a local linear estimate with a nearest-neighbour bandwidth, whose span is chosen in order to minimise the AIC. In contour and HDR plots, the dashed line indicates the main diagonal, the asterisks represent the modes.

current values, the lags and the leads are considered in the regression.

In the present context, the growth rate of the property crime rate is regressed on the growth rates of personal per capita income and state police rates, current, lagged and leaded:

$$g_{i,t}^c = \alpha + \sum_{j=-l}^l (\beta_j g_{i,t+j}^y + \gamma_j g_{i,t+j}^p) + \varepsilon_{i,t} \quad (3.11)$$

where $g_{i,t}^x$ is the growth rate of the variable x between time $t - 1$ and t in state i , whereas l represents the number of lags and leads considered in the regressions.¹⁴

The results of the estimates are presented in Table 3.2: in particular, the three columns show the estimates with one, two and three lags/leads, respectively. The period considered is from 1971 to 2010 for the 48 conterminous US states (1920 observations in total) in all specifications.¹⁵ The estimated coefficients are substantially constant across the three specifications. For the next analysis, the fitted values from the third regression are selected, although the subsequent results seem robust and are not heavily affected by this choice.

The second step of the procedure consists in the accumulation of these fitted values, state by state, to obtain the time-varying trend paths explained by the conditioning variables:

$$g_{i,t}^* = \sum_{j=1}^t \hat{g}_{i,j}^c \quad (3.12)$$

This determines up to a multiplicative time-invariant level,¹⁶ given by the initial region-specific value of crime, the component for each state explained

¹⁴The inclusion of leads might not solve completely the endogeneity problem due to the many possible channels of reversed causality between dependent and independent variables: this means that the following results shall be interpreted with caution and on a descriptive basis.

¹⁵Out-of-sample values have been used to compute the lags and leads at the beginning and at the end of the period considered.

¹⁶In Quah's (1996b) procedure the accumulation of fitted values determines up to an additive constant level the component explained by the conditioning variables because the variable of interest in that paper is in logarithm.

Conditioning Variables	(1)	(2)	(3)
g_{t-3}^y			0.3755 (0.0562)
g_{t-2}^y		0.6378 (0.0676)	0.5653 (0.0694)
g_{t-1}^y	0.4261 (0.0731)	0.3355 (0.0755)	0.3819 (0.0780)
g_t^y	-0.5208 (0.0678)	-0.4615 (0.0652)	-0.4307 (0.0643)
g_{t+1}^y	-0.4308 (0.0633)	-0.3760 (0.0653)	-0.3467 (0.0635)
g_{t+2}^y		0.1025 (0.0632)	0.0545 (0.0630)
g_{t+3}^y			0.1828 (0.0625)
g_{t-3}^p			0.0206 (0.0131)
g_{t-2}^p		0.0126 (0.0155)	0.0115 (0.0164)
g_{t-1}^p	0.0371 (0.0186)	0.0287 (0.0195)	0.0246 (0.0197)
g_t^p	0.0249 (0.0153)	0.0172 (0.0155)	0.0186 (0.0149)
g_{t+1}^p	0.0068 (0.0133)	0.0100 (0.0127)	0.0126 (0.0124)
g_{t+2}^p		0.0017 (0.0144)	0.0098 (0.0144)
g_{t+3}^p			0.0178 (0.0137)
Constant	0.0055 (0.0021)	-0.0064 (0.0023)	-0.0155 (0.0027)
Observations	1920	1920	1920
Sum of Coefficients: Income	-0.5255	0.2383	0.7825
Sum of Coefficients: Police	0.0688	0.0702	0.1156
R^2	0.1182	0.1825	0.2117

Table 3.2: Conditioning regressions. *Notes:* each column reports estimates of the coefficients in the projection. Numbers in parentheses are the White heteroskedasticity-consistent standard errors. The dependent variable is the growth rate of property crime rate while the conditioning variables are the current, lagged and leaded growth rates of personal per capita income and state police rates. The years from 1971 to 2010 are considered for the 48 conterminous US states (1920 observations in total): out-of-sample values have been used to compute the lags and leads at the beginning and at the end of the period considered.

by income and police: as in Quah (1996b), it is assumed that this state-specific multiplicative level is equal to a linear combination of the time averages of income \bar{y}_i and police \bar{p}_i . The parameters of this linear combination are determined by solving the following minimisation problem:¹⁷

$$\min_{a,b} \sum_i \sum_t [c_{i,t} - (a\bar{y}_i + b\bar{p}_i) (1 + g_{i,t}^*)]^2 \quad (3.13)$$

The difference between actual and fitted paths in squared brackets can be interpreted as the conditional or unexplained component of property crime and it is used in the following distribution dynamics exercise: in fact, Figure 3.11 and 3.12 are obtained by applying the distribution dynamics analysis to the unexplained component for the periods 1971-2010 and 1981-2010, respectively. The conditional convergence is made evident by the noticeable clockwise rotation of the estimated probability mass in both figures. Moreover, any sign of bimodality is completely disappeared from the ergodic distribution, which is also more concentrated than the initial and final one. Thus, the divergence in the number of state police forces and the increasing income inequality started in the 1980s explain well the tendency towards a bimodal shape in the property crime distribution.

3.8 Concluding Remarks

The importance of analysing the convergence of crime rates, as stated by Cook and Winfield (2013), is related to the existence of a possible national crime trend and whether there are movements towards it. Moreover, the analysis of convergence helps in choosing between competing sociological theories, like the modernization and the conflict theories (LaFree, 2005): in fact, according to the modernization view, crime rates should converge given the spread of developments and advances across regions, whereas the

¹⁷Again, the difference with respect to Quah's (1996b) procedure is related to the logarithm transformation adopted in that study.

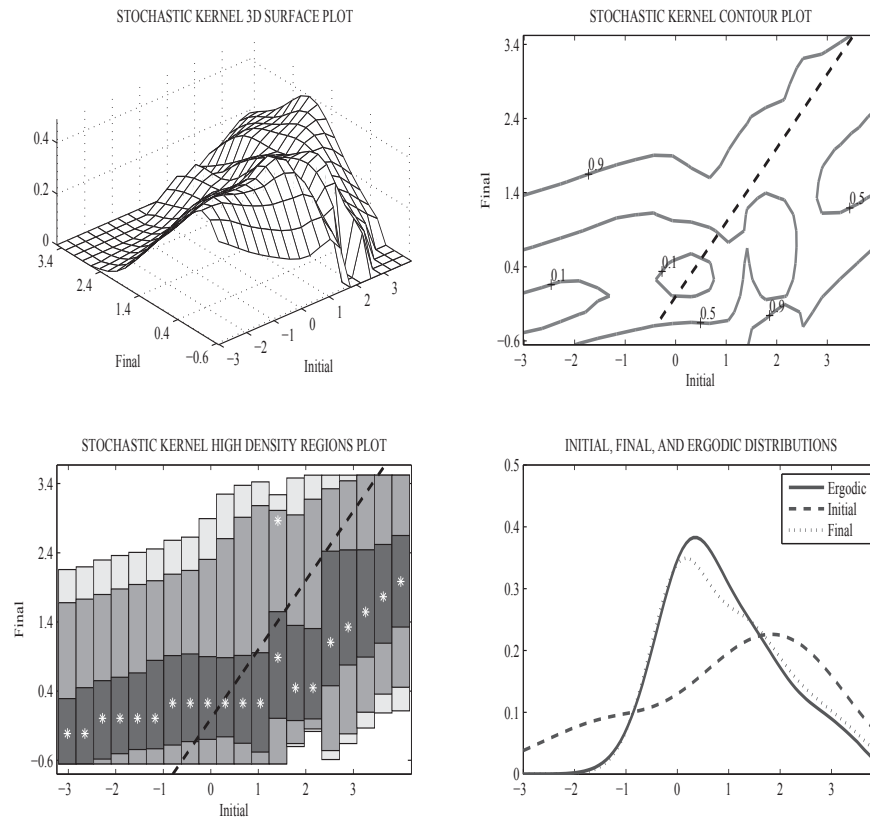


Figure 3.11: Distribution dynamics analysis of property crime rates for the period 1971-2010 conditioning on income and police. A three-dimensional plot of the estimated stochastic kernel (top-left); the corresponding contour plot, highlighting the contours at the 90%, 50% and 10% level (top-right); the Highest Density Regions (HDR) plot (bottom-left); a graph comparing the initial year and the final year distribution with the ergodic distribution (bottom-right). *Notes:* estimates of the stochastic kernel adopt a nearest-neighbour bandwidth in the initial year dimension with a span equal to 0.3, a Normal Scale (Silverman, 1986) bandwidth in the final year dimension and a Gaussian kernel. The mean bias adjustment (Hyndman *et al.*, 1996) is obtained using a local linear estimate with a nearest-neighbour bandwidth, whose span is chosen in order to minimise the AIC. In contour and HDR plots, the dashed line indicates the main diagonal, the asterisks represent the modes.

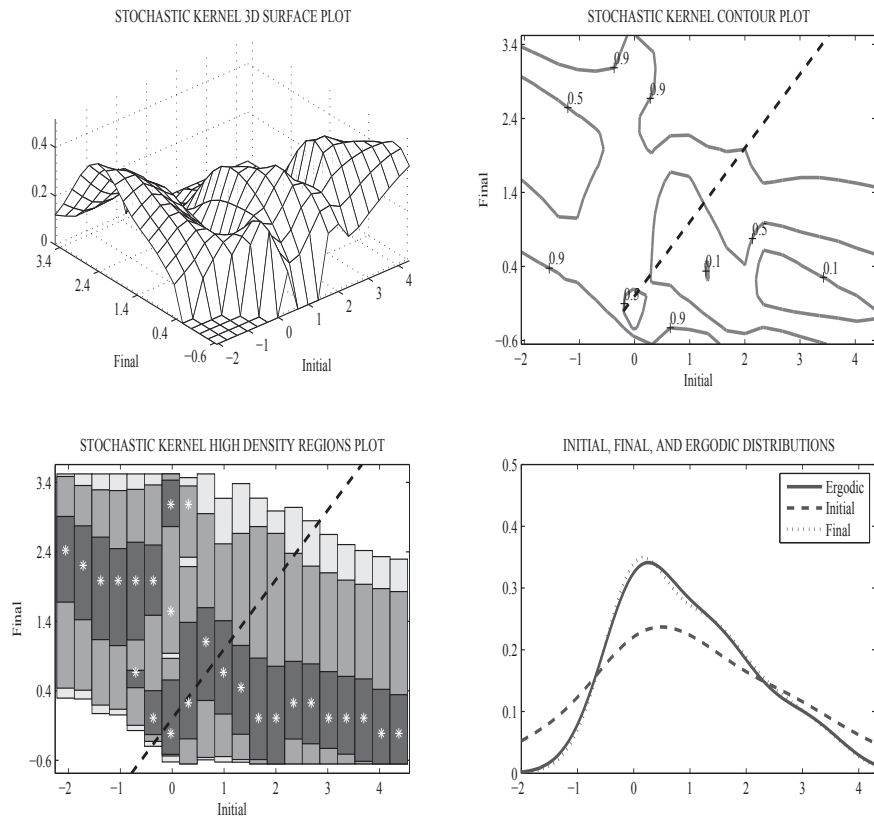


Figure 3.12: Distribution dynamics analysis of property crime rates for the period 1981-2010 conditioning on income and police. A three-dimensional plot of the estimated stochastic kernel (top-left); the corresponding contour plot, highlighting the contours at the 90%, 50% and 10% level (top-right); the Highest Density Regions (HDR) plot (bottom-left); a graph comparing the initial year and the final year distribution with the ergodic distribution (bottom-right). *Notes:* estimates of the stochastic kernel adopt a nearest-neighbour bandwidth in the initial year dimension with a span equal to 0.3, a Normal Scale (Silverman, 1986) bandwidth in the final year dimension and a Gaussian kernel. The mean bias adjustment (Hyndman *et al.*, 1996) is obtained using a local linear estimate with a nearest-neighbour bandwidth, whose span is chosen in order to minimise the AIC. In contour and HDR plots, the dashed line indicates the main diagonal, the asterisks represent the modes.

conflict theory predicts their divergence, arguing that these developments have uneven speed in the different regions.

The proposed theoretical model reproduces the emergence of two distinct phases in the dynamics of property crime distribution when spatial units are affected by strong income shocks generating greater inequality: a period of convergence followed by the divergence of crime rates. This scenario fits the situation of the US states, because economic disparities were exacerbated in those regions, starting from the 1980s.

This theoretical prediction is confirmed by the descriptive analysis presented in this paper. In fact, using the distribution dynamics methodology, two different patterns are identified during the period 1971-2010 for the property crime distribution: a phase of strong convergence (1971-1980), followed by a period of divergence and a tendency towards bimodality (1981-2010). These two distinct phases, to the best of our knowledge, have not been highlighted by the existing literature.

Moreover, the contemporaneous divergence of personal per capita income and of state police rates can account for the observed dynamics of property crime rates: in fact, conditioning on income per capita and state police, the distribution of property crime does not exhibit a bimodal shape, thus indicating the presence of conditional convergence.

An important policy implication that can be derived from the analysis is as follows. The theoretical framework suggests that significant income disparities are translated into different concentrations of crime through the opportunity cost and the police channel. Moreover, given that poor states have lower resources to fight crime, they are likely to exhibit higher crime rates too. Since the presence of crime discourages investments and lowers income, these states are trapped in a vicious circle. Therefore, mitigating the effects of inequality with cross-state compensations, in terms of financial and police resources, may help avoiding both the concentration of crime activities in specific regions and the emergence of self-reinforcing gaps between

poor and rich states.

Acknowledgments

I am grateful to Prof. Paolo Pellizzari and Prof. Stefano Magrini for their extremely useful comments and suggestions which have greatly improved the contents of each chapter of the present PhD dissertation. I thank Prof. Margherita Gerolimetto and Prof. Stefano Magrini for the code used to implement the distribution dynamics analysis performed in the third chapter. I also thank Prof. Ugo Fratesi, Prof. Carlo Giupponi and Prof. Matteo Richiardi, all the participants in the RODEO seminars in Venice, the 8th Ruhr Graduate School Doctoral Conference in Essen, the 20th Spring Meeting of Young Economists in Ghent, the 1st Ca' Foscari and Groningen PhD Workshop in Groningen, and the anonymous referees of PLoS ONE and *Urban Studies* for interesting critical discussions. Special thanks to my parents and grandparents for their invaluable support.

Bibliography

- [1] Acemoglu, D., and J. A. Robinson (2001). “A Theory of Political Transitions.” *American Economic Review*, 91(4): 938-63.
- [2] Anselin, L. (1995). “Local Indicators of Spatial Association-LISA.” *Geographical Analysis*, 27(2): 93-115.
- [3] Baltagi, B. H. (2006). “Estimating an Economic Model of Crime Using Panel Data from North Carolina.” *Journal of Applied Econometrics*, 21(4): 543–547.
- [4] Barro, R. J. (1991). “Economic Growth in a Cross Section of Countries.” *Quarterly Journal of Economics*, 106(2): 407-443.
- [5] Barro, R. J., and X. Sala-i-Martin (1991). “Convergence Across States and Regions.” *Brooking Papers on Economic Activity*, 1991(1): 107-182.
- [6] Barro, R. J., and X. Sala-i-Martin (1992). “Convergence.” *Journal of Political Economy*, 100(2): 223-251.
- [7] Baumol, W. J. (1986). “Productivity Growth, Convergence, and Welfare: What the Long-Run Data Show.” *American Economic Review*, 76(5): 1072-1085.
- [8] Becker, G. S. (1968). “Crime and Punishment: An Economic Approach.” *Journal of Political Economy*, 76(2): 169-217.

- [9] Branas, C. C., T. S. Richmond, D. P. Culhane, T. R. Ten Have, and D. J. Wiebe (2009). "Investigating the Link between Gun Possession and Gun Assault." *American Journal of Public Health*, 99(11): 2034-2040.
- [10] Cohen, L. E., and M. Felson (1979). "Social Change and Crime Rate Trends: A Routine Activities Approach." *American Sociological Review*, 44(4): 588-608.
- [11] Collier, P., and A. Hoeffler (1998). "On Economic Causes of Civil War." *Oxford Economic Papers*, 50(4): 563-73.
- [12] Collier, P., and A. Hoeffler (2004). "Greed and Grievance in Civil War." *Oxford Economic Papers*, 56(4): 563-95.
- [13] Cook, J., and S. Cook (2011). "Are US Crime Rates Really Unit Root Processes?" *Journal of Quantitative Criminology*, 27(3): 299-314.
- [14] Cook, S., and D. Watson (2013). "Breaks and Convergence in U.S. Regional Crime Rates: Analysis of Their Presence and Implications." *Social Sciences*, 2(3): 180-190.
- [15] Cook, S., and T. Winfield (2013). "Crime across the States: Are US Crime Rates Converging?" *Urban Studies*, 50(9): 1724-1741.
- [16] Cornwell, C., and W. N. Trumbull (1994). "Estimating the Economic Model of Crime with Panel Data." *Review of Economics and Statistics*, 76(2): 360-366.
- [17] Cummings, P., T. D. Koepsell, D. C. Grossman, J. Savarino, and R. S. Thompson (1997). "The Association between the Purchase of a Handgun and Homicide or Suicide." *American Journal of Public Health*, 87(6): 974-978.
- [18] Davies, J. C. (1962). "Toward a Theory of Revolution." *American Sociological Review*, 27(1): 5-19.

- [19] Donohue, J. J., and S. D. Levitt (2001). "The Impact of Legalized Abortion on Crime." *Quarterly Journal of Economics*, 116(2): 379-420.
- [20] Ellis, C. J., and J. Fender (2011). "Information Cascades and Revolutionary Regime Transitions." *Economic Journal*, 121(553): 763-792.
- [21] Epstein, J. M. (2002). "Modeling Civil Violence: An Agent-Based Computational Approach." *Proceedings of the National Academy of Sciences*, 99(3): 7243-7250.
- [22] Fearon, J. D., and D. D. Laitin (2003). "Ethnicity, Insurgency, and Civil War." *American Political Science Review*, 97(1): 75-90.
- [23] Gard-Murray, A. S., and Y. Bar-Yam (2015). "Complexity and the Limits of Revolution: What Will Happen to the Arab Spring?." *Conflict and Complexity*, Springer, New York: 281-292.
- [24] Gerolimetto, M., and S. Magrini (2014). "A Novel Look at Long-Run Convergence Dynamics in the United States." *International Regional Science Review*: 1-29.
- [25] Goldstone, J. A. (2001). "Toward a Fourth Generation of Revolutionary Theory." *Annual Review of Political Science*, 4: 139-187.
- [26] Goldstone, J. A. (2011). "Understanding the Revolutions of 2011. Weakness and Resilience in Middle Eastern Autocracies." *Foreign Affairs*, 90(3): 8-16.
- [27] Gould, E. D., B. A. Weinberg and D. B. Mustard (2002). "Crime Rates and Local Labor Market Opportunities in the United States: 1979-1997." *Review of Economics and Statistics*, 84(1): 45-61.
- [28] Granovetter, M. (1978). "Threshold Models of Collective Behavior." *American Journal of Sociology*, 83(6): 1420-1443.

- [29] Grassel, K. M., G. J. Wintemute, M. A. Wright, and M. P. Romero (2003). “Association between Handgun Purchase and Mortality from Firearm Injury.” *Injury Prevention*, 9(1): 48-52.
- [30] Grazzini, J. (2012). “Analysis of the Emergent Properties: Stationarity and Ergodicity.” *Journal of Artificial Societies and Social Simulation*, 15(2): 7.
- [31] Grazzini, J., and M. Richiardi (2015) “Estimation of Ergodic Agent-Based Models by Simulated Minimum Distance.” *Journal of Economic Dynamics and Control*, 51: 148-165.
- [32] Greenberg, D. F. (2001). “Time Series Analysis of Crime Rates.” *Journal of Quantitative Criminology*, 17(4): 291–327.
- [33] Hartley, J. E. (1996). “Retrospectives: The Origins of the Representative Agent.” *Journal of Economic Perspectives*, 10(2): 169-177.
- [34] Hayes, R., and R. Hayes (2014). “Agent-Based Simulation of Mass Shootings: Determining How to Limit the Scale of a Tragedy.” *Journal of Artificial Societies and Social Simulation*, 17(2): 5.
- [35] Hegel, G.W.F. (1807 [1910]). *The Phenomenology of Mind*. London: Sonnenschein.
- [36] Hemenway, D. (2006). *Private Guns, Public Health*. University of Michigan Press.
- [37] Hemenway, D., and M. Miller (2000). “Firearm Availability and Homicide Rates Across 26 High-Income Countries”. *Journal of Trauma and Acute Care Surgery*, 49(6): 985–988.
- [38] Hyndman, R. J. (1996). “Computing and Graphing Highest Density Regions.” *American Statistician*, 50(2): 120-126.

- [39] Hyndman, R. J., D. M. Bashtannyk and G. K. Grunwald (1996). "Estimating and Visualizing Conditional Densities." *Journal of Computational and Graphical Statistics*, 5(4): 315–336.
- [40] Jacobs, J. B. (2002) *Can Gun Control Work?* Oxford University Press.
- [41] Kapuscinski, C. A., J. Braithwaite, and B. Chapman (1998). "Unemployment and Crime: Toward Resolving the Paradox." *Journal of Quantitative Criminology*, 14(3): 215–243.
- [42] Kellermann, A. L., F. P. Rivara, N. B. Rushforth, J. G. Banton, D. T. Reay, J. T. Francisco, ..., and G. Somes (1993). "Gun Ownership as a Risk Factor for Homicide in the Home." *New England Journal of Medicine*, 329(15): 1084-1091.
- [43] Kennedy, B. P., I. Kawachi, D. Prothrow-Stith, K. Lochner, and V. Gupta (1998). "Social Capital, Income Inequality, and Firearm Violent Crime." *Social Science and Medicine*, 47(1): 7–17.
- [44] Kim, J. W., and R. A. Hanneman (2011). "A Computational Model of Worker Protest." *Journal of Artificial Societies and Social Simulation*, 14(3): 1.
- [45] Kirman, A. P. (1992). "Whom or What Does the Representative Individual Represent?" *Journal of Economic Perspectives*, 6(2): 117-136.
- [46] Kleck, G., and M. Gertz (1995). "Armed Resistance to Crime: the Prevalence and Nature of Self-Defense with a Gun." *Journal of Criminal Law and Criminology*, 86(1): 150–187.
- [47] Kleck, G., and M. Hogan (1999). "National Case-Control Study of Homicide Offending and Gun Ownership." *Social Problems*, 46(2): 275-293.
- [48] Kuran, T. (1989). "Sparks and Prairie Fires: A Theory of Unanticipated Political Revolution." *Public Choice*, 61(1): 41-74.

- [49] Kuran, T. (1991). "The East European Revolution of 1989: Is it Surprising That We Were Surprised?" *American Economic Review*, 81(2): 121-125.
- [50] Kuran, T. (1995). "The Inevitability of Future Revolutionary Surprises." *American Journal of Sociology*, 100(6): 1528-1551.
- [51] LaFree, G. (2005). "Evidence for Elite Convergence in Cross-National Homicide Victimization Trends, 1956 to 2000." *Sociology Quarterly*, 46(1): 191-211.
- [52] Lagi, M., K. Z. Bertrand, and Y. Bar-Yam (2011). "The Food Crises and Political Instability in North Africa and the Middle East." arXiv:1108.2455.
- [53] Leeson, P.T. (2010). "Rational Choice, Round Robin, and Rebellion: An Institutional Solution to the Problems of Revolution." *Journal of Economic Behavior and Organization*, 73(3): 297-307.
- [54] Levitt, S. D. (2002). "Using Electoral Cycles in Police Hiring to Estimate the Effects of Police on Crime: Reply." *American Economic Review*, 92(4): 1244-1250.
- [55] Levitt, S. D. (2004). "Understanding Why Crime Fell in the 1990s: Four Factors that Explain the Decline and Six that Do Not." *Journal of Economic Perspectives*, 18(1): 163-190.
- [56] Lichbach, M. I. (1994). Rethinking Rationality and Rebellion: Theories of Collective Action and Problems of Collective Dissent. *Rationality and Society*, 6(1): 8-39.
- [57] Lichbach, M. I. (1995). *The Rebel's Dilemma: Collective Action and Collective Dissent*. Ann Arbor: University of Michigan Press.
- [58] Lichbach, M. I. (1996). *The Cooperator's Dilemma: Social Order and Collective Action*. Ann Arbor: University of Michigan Press.

- [59] Loader, C. R. (1999). *Local Regression and Likelihood*. New York: Springer.
- [60] Lott, J. (2010). *More Guns, Less Crime: Understanding Crime and Gun Control Laws*. University of Chicago Press.
- [61] Machin, S., and C. Meghir (2004). “Crime and Economic Incentives.” *Journal of Human Resources*, 39(4): 958-979.
- [62] Makowsky, M., and J. Rubin (2013). “An Agent-Based Model of Centralized Institutions, Social Network Technology, and Revolution.” *PLoS ONE*, 8(11): e80380.
- [63] Marshall, A. (1920 [1961]). *Principles of Economics*. London: Macmillan.
- [64] Marvell, T. B., and C. E. Moody (1996). “Specification Problems, Police Levels, and Crime Rates.” *Criminology*, 34(4): 609-646.
- [65] Marvell, T. B., and C. E. Moody (2001). “The Lethal Effects of Three-Strikes Laws.” *Journal of Legal Studies*, 30(1): 89–106.
- [66] McCall, P. L., K. F. Parker, and J. M. MacDonald (2008). “The Dynamic Relationship Between Homicide Rates and Social, Economic, and Political Factors from 1970 to 2000.” *Social Science Research*, 37(3): 721–735.
- [67] Miguel, E., S. Satyanath, and E. Sergenti (2004). “Economic Shocks and Civil Conflict: An Instrumental Variables Approach.” *Journal of Political Economy*, 112(4): 725–753.
- [68] Paternoster, R., and S. D. Bushway (2001). “Theoretical and Empirical Work on the Relationship Between Unemployment and Crime.” *Journal of Quantitative Criminology*, 17(4): 391–407.

- [69] Quah, D. T. (1993a). “Galton’s Fallacy and Tests of the Convergence Hypothesis.” *Scandinavian Journal of Economics*, 95(4): 427–443.
- [70] Quah, D. T. (1993b). “Empirical Cross-Section Dynamics in Economic Growth.” *European Economic Review*, 37(2-3): 426–434.
- [71] Quah, D. T. (1996a). “Empirics for Economic Growth and Convergence.” *European Economic Review*, 40(6): 1353–1375.
- [72] Quah, D. T. (1996b). “Convergence Empirics across Economies with (Some) Capital Mobility.” *Journal of Economic Growth*, 1(1): 95–124.
- [73] Quah, D. T. (1997). “Empirics for Growth and Distribution: Stratification, Polarization, and Convergence Clubs.” *Journal of Economic Growth*, 2(1): 27–59.
- [74] Raphael, S., and R. Winter-Ebmer (2001). “Identifying the Effect of Unemployment on Crime.” *Journal of Law and Economics*, 44(1): 259–283.
- [75] R Core Team (2014). *R: A Language and Environment for Statistical Computing*. R Foundation for Statistical Computing, Vienna, Austria. URL <http://www.R-project.org/>.
- [76] Rennison, C. M. (2009). “Crime Reports and Statistics.” In Miller, J. (Ed.), *21st Century Criminology: A Reference Handbook*, Thousand Oaks: SAGE Publications: 383-391.
- [77] Rosenfeld, R., and R. Fornago (2007). “The Impact of Economic Conditions on Robbery and Property Crime: the Role of Consumer Sentiment.” *Criminology*, 45(4): 735–769.
- [78] Rubin, J. (2014). “Centralized Institutions and Cascades.” *Journal of Comparative Economics*, 42(2): 340-357.

- [79] Sala-i-Martin, X. (1996). "Regional Cohesion: Evidence and Theories of Regional Growth and Convergence." *European Economic Review*, 40(6): 1325-1352.
- [80] Saltelli, A., M. Ratto, T. Andres, F. Campolongo, J. Cariboni, D. Gatelli, M. Saisana and S. Tarantola (2008). *Global Sensitivity Analysis: The Primer*, John Wiley and Sons.
- [81] Shoemith, G. L. (2010). "Four Factors that Explains both the Raise and Fall of US Crime, 1970-2003." *Applied Economics*, 42(23): 2957-2973.
- [82] Silver, M. (1974). "Political Revolution and Repression: An Economic Approach." *Public Choice*, 17(1): 63-71.
- [83] Silverman, B. W. (1981). "Using Kernel Density Estimates to Investigate Multimodality." *Journal of the Royal Statistical Society, Series B*, 43(1): 97-99.
- [84] Silverman, B. W. (1986). *Density Estimation for Statistics and Data Analysis*. London: Chapman & Hall.
- [85] Skocpol, T. (1979). *States and Social Revolutions: A Comparative Analysis of France, Russia, and China*. Cambridge: Cambridge University Press.
- [86] Smith, K. B. (1997). "Explaining Variation in State-Level Homicide Rates: Does Crime Policy Pay?" *Journal of Politics*, 59(2): 350-367.
- [87] Taleb, N. N., and G. F. Treverton (2015). "The Calm Before the Storm: Why Volatility Signals Stability, and Vice Versa." *Foreign Affairs*, 94(1): 86-95.
- [88] Tullock, G. (1971). "The Paradox of Revolutions." *Public Choice*, 11(1): 89-99.

- [89] Wiebe, D. J. (2003). "Homicide and Suicide Risks Associated with Firearms in the Home: a National Case-Control Study." *Annals of Emergency Medicine*, 41(6): 771-782.
- [90] Wilensky, U. (1999). NetLogo. Center for Connected Learning and Computer-Based Modeling, Northwestern University, Evanston, IL. URL <http://ccl.northwestern.edu/netlogo/>.
- [91] Wilensky, U. (2004). "NetLogo Rebellion Model." Evanston, IL: Center for Connected Learning and Computer-Based Modeling, Northwestern University. URL <http://ccl.northwestern.edu/netlogo/models/Rebellion>.
- [92] Wodarz, D., and N. L. Komarova (2013). "Dependence of the Firearm-Related Homicide Rate on Gun Availability: A Mathematical Analysis." *PLoS ONE*, 8(7): e71606.